LBL-6841

To be presented at the Fall Meeting of the Western States Section of the Combustion Institute, Stanford, CA, October 17 - 18, 1977

Energy and Environment Division

Catalyzed Combustion in a Flat Plate Boundary Layer I. Experimental Measurements and Comparison with Numerical Calculations

R. Robben, R. Schefer, V. Agrawal, and I. Namer

September 1977

Lawrence Berkeley Laboratory University of California/Berkeley

Prepared for the U.S. Energy Research and Development Administration under Contract No. W-7405-ENG-48

LBL-6841
c.1

CATALYZED COMBUSTION IN A FLAT PLATE BOUNDARY LAYER

I. EXPERIMENTAL MEASUREMENTS AND COMPARISON WITH NUMERICAL CALCULATIONS[†] *

F. Robben, R. Schefer,[††] V. Agrawal, I. Namer

September 1977

[†]To be presented at the Fall Meeting, Western States Section of The Combustion Institute, October 17-18, Stanford, California.

*This work was primarily supported by ERDA, Division of Conservation Research and Technology. The experimental equipment and technique were also jointly supported by the Air Force Office of Scientific Research and ERDA, Division of Basic Energy Sciences.

[††]NSF Energy Related Postdoctoral Fellow.

CATALYZED COMBUSTION IN A FLAT PLATE BOUNDARY LAYER

I. EXPERIMENTAL MEASUREMENTS AND COMPARISON WITH NUMERICAL CALCULATIONS[†] *

F. Robben, R. Schefer,[††] V. Agrawal, I. Namer

September 1977

[†]To be presented at the Fall Meeting, Western States Section of The Combustion Institute, October 17-18, Stanford, California.

*This work was primarily supported by ERDA, Division of Conservation Research and Technology. The experimental equipment and technique were also jointly supported by the Air Force Office of Scientific Research and ERDA, Division of Basic Energy Sciences.

[††]NSF Energy Related Postdoctoral Fellow.

ABSTRACT

A classic fluid mechanics boundary layer problem, flow over a sharp leading edge flat plate, has been used to study the effect of a heated surface on combustion in lean hydrogen-air mixtures. The velocity and density profiles of the boundary layer have been measured with laser Doppler velocimetry and Rayleigh scattering, respectively. Preliminary measurements on a silicon dioxide "non-catalytic" surface indicate neither boundary layer nor surface combustion for wall temperatures up to 1250 K. Measurements on a platinum catalytic surface indicate that, at a surface temperature of 1000 K, not only is there significant surface combustion but that homogeneous combustion in the boundary layer is induced by active species generated at the catalytic surface.

INTRODUCTION

The use of surface catalysis to complete the oxidation of unburned hydrocarbons and carbon monoxide from automotive engines has become a successful, practical application of catalysis to reduce combustion generated pollution. Besides this well known example to clean up the exhaust gases from combustion, there is considerable promise in using surface catalysis directly in the combustion process in order to reduce the associated pollution. Most emphasis has been directed at lean premixed combustion, where the reduced combustion temperature can effectively make the formation of nitric oxide by thermal reactions negligible[1,2]. Surface catalysis is very effective in this application by initiating and speeding up the combustion reactions so that complete combustion can be attained under conditions where stable combustion is difficult or impossible to achieve using conventional combustors.

This application is most promising for gas turbine combustors, where a quite lean overall fuel-air ratio is necessary in order to limit the temperature of the inlet turbine blades. Considerable research and development work has been carried out[3-6]. As an example of the state of the art, satisfacotry life tests of 1000 hours at a temperature close to 1500^{o} K have been carried out, using a commercial grade of diesel as fuel[7].

Besides gas turbine combustors, work has also been carried out on the application of catalyzed combustion to industrial boilers, space and hot water heaters, and industrial process heaters[8,9]. Since there is a wide variety of possible systems that could be engineered using catalysis, the application looks very promising and is presently an active area of research and development.

The principal objective of the present research is to improve the understanding of high temperature heterogeneous catalysis of combustion reactions and the coupling with the homogeneous reactions and the fluid mechanics. From a practical standpoint, the anticipated results should be useful in the evaluation and application of catalysis technology to combustors.

Combustion in the boundary layer of a heated flat plate, with a free stream flow of premixed fuel and air at ambient temperature and pressure involves most of the important physical and chemical processes of catalytic combustion systems while providing a suitable geometry for experimental study and numerical calculations. The present experiments have concentrated on two optical diagnostic techniques, laser Doppler velocimetry for measurement of the velocity distribution in the boundary layer and Rayleigh scattering for measurement of the density distribution. These techniques are non-perturbing to the flow and combustion process and are capable of good time and three-dimensional

spatial resolution. They were also chosen in order to develop their application to the study of combustion phenomena; in particular, these techniques have promise in the study of boundary layer combustion under turbulent conditions. The boundary layer density profiles have also been photographed using a variant of the Schlieren technique known as deflection mapping, which has given considerable insight into the combustion process.

In the remainder of this paper the experimental facility and diagnostics are described and some preliminary results obtained over SiO and SiO_2 "non-catalytic" surfaces and a platinum "catalytic" surface are discussed. The parallel numerical study of boundary layer flow and combustion is described in a companion paper[10].

EXPERIMENTAL FACILITY

Open Jet Flow

For experimental convenience, the flow over a sharp leading edge flat plate is created in an open, atmospheric pressure jet of premixed fuel and air. Figure 1 shows schematically the open jet flow and flat plate and indicates the development of the boundary layer on the flat plate and the mixing of the jet with the ambient air. Figure 2 shows the arrangement of the flow (directed vertically upwards), the flat plate and the laser diagnostics. The stagnation chamber is 20 cm in diameter and can be fitted with 2.5 or 5 cm diameter nozzles. It has three internal screens and produces

a uniform, low turbulence flow of air or combustible mixture. Lower flow rates of gases are metered by calibrated rotameters, larger air flow rates are metered using a standard orifice gauge and water manometer. The house air supply is passed through a dryer and filter combination which eliminates most of the particulate matter. The entire stagnation chamber is mounted on a three-dimensional traverse mechanism (adapated from a milling machine) and has 0.001 cm positioning sensitivity.

Heated Flat Plate

Several types of sharp leading edge, heated flat plates have been tested. Thin metal sheets were unsatisfactory since a sufficiently flat surface could not be obtained. A thick stainless steel plate heated with silicon carbide rods was used for some preliminary measurements, but had the disadvantages of behaving like a wedge in the flow, as well as having unknown catalytic surface properties. In particular, the wedge type flow greatly disturbed the open jet and made accurate numerical computation of the flow field difficult. Finally, a thin quartz plate with vacuum deposited platinum heating strips was constructed and found satisfactory.

Figure 3 shows the present design of the flat plates. They are made of quartz sheet, 1.5 mm thick and 75 mm square, with a sharp leading edge of 2° included angle. Five platinum heating strips are oriented perpendicular to the flow, with a relatively narrow strip near the

leading edge. Electrical power is individually controlled to each of these strips and as a result a reasonably uniform plate surface temperature can be maintained.

In order to reduce the interference of surface scattering of the laser beam with the Rayleigh scattering in the boundary layer, important when measurements are being made close to the plate, it has been found advantageous to have a small bend, about 2°, in the center of the plate. The Rayleigh scattering measurements are made in the shadow of this bend. To produce this bend the plate is placed in a graphite mold in a vacuum furnace and heated to the softening point of quartz.

The platinum heating strips are then evaporated on the plate, while heating the plate simultaneously to increase the adhesion. The central region of the plate is coated to a thickness of 0.3 to 0.5 microns, while the outer edges are coated with about 2.5 times this thickness. This keeps the outer edges of the plate cool so that gold foil can be used to make electrical contact with the stainless steel fingers, as shown in Fig. 3. While the platinum adhered quite satisfactorily in an initial test, we have since had considerable trouble with adhesion. The platinum would, on occasion, bubble up and separate from the quartz substrate. Cleaning the surface of the quartz by "sand blasting" with quartz particles prior to coating greatly improved the adhesion between the quartz substrate and the platinum strips. The lifetime of the platinum coating, at temperatures up to 1000 C, has been of the order of 30 hours.

In order to obtain a "non-catalytic" surface, silicon monoxide, and later silicon dioxide, were evaporated over the platinum coating. These coatings adhered satisfactorily and greatly reduced the catalytic activity from that of bare platinum. We also intend to try an evaporated aluminum oxide coating as a non-catalytic surface. To produce a catalytic surface typical of commercial combustion catalysts (rather than vacuum deposited platinum), a coating of activated alumina has been deposited on the surface with good results.* In future tests this activated alumina will be impregnated with various commercially used catalysts.

Accurate measurement of surface temperature is important. At present a disappearing filament type optical pyrometer is used, and an emissivity estimate of 0.45 for the rather rough platinum surface was made. With such a pyrometer, operating at 0.65 micron wavelength, the lowest brightness temperature which can be measured is approximately 700 C. Future plans include measurement of the surface emissivity, and use of an infrared pyrometer in order to measure lower temperatures.

Measurement of temperature is also possible from the resistivity of the platinum strips. To measure the resistance properly, with separate voltage leads to the central heated region, appears too complex at present. However, the ratio of the overall voltage and current is closely

*This was carried out by W.B. Retallick of Oxy-Catalyst, Inc.

related to the central region resistance. Lower temperatures have been measured this way, and the electrical power input can be measured to obtain information on the heat transfer to the surface.

Laser Velocimeter

The laser Doppler velocimeter is of the intersecting dual-beam type with real fringes[11]. A cube type beam splitter, consisting of two 90° equilateral prisms cemented along the hypotenense, is used. The hypotenense of one prism is coated for 50% reflectivity. This splits the laser beam into two beams with equal optical path length and variable beam separation, where parallelism can be adjusted by rotating the cube. These two beams are focussed by a single lens and intersect at the measurement volume. The diameter of the laser beams was determined by measuring the scattering from a 10 micron diameter wire as it was traversed across the beams. It was found that the two beams did not intersect at their waist diameters, due to the spherical aberration of the focussing lens, when the beams were initially parallel. This was corrected by rotating the cube beam splitter so that the nominally parallel beams diverged slightly.

The scattering from the intersection region was detected at a 30° angle from the forward direction. The scattering detector consisted of a 55 mm focal length camera lens which imaged a pinhole on the intersection region, and an RCA type 931 A photomultiplier. The scattering bursts could be observed directly on an oscilloscope, and photographed.

The frequency of the bursts was also determined by a Thermal Systems Model 1090 frequency tracker which converted each burst into a voltage proportional to the frequency, or particle velocity.

Aluminum oxide particles of nominally 2.0 micron diameter were introduced into the air supply prior to the stagnation chamber. The particles were mixed with water and a series of air jets near the water surface were used to stir and atomize the water-particle mixture. This technique was moderately satisfactory; particle counting rates varying from 300 to 1000 sec^{-1} were attained. However, a small but unknown amount of water was carried into the combustible mixture, and the number of particles decreased considerably after entering the heated region of the flow where the condensed water droplets were evaporated. To eliminate these problems, a particle generator based on the smoke from a burning magnesium ribbon has been constructed and is currently being tested.

Rayleigh Scattering

Rayleigh scattering refers to the light scattered from gas molecules without any shift in wavelength[12]. The intensity is proportional to the gas density, if one neglects the small effect of changes in chemical composition, and gives approximately the same information as an interferometric measurement of gas density. The principal advantages over interferometric techniques[13] is that it measures the density at a single point rather than integrating along the line of sight,

which makes it particularly suitable for measurement of three-dimensional geometries. Further, with moderate powered lasers the intensity is sufficient such that adequate time resolution and signal-to-noise ratio can be obtained for studies of fluid mechanical and combustion turbulence[14]. The principal disadvantage, compared to an interferometric photograph, is that the density is measured at only one point at a time. This makes it difficult to obtain satisfactory measurements of an entire flow field.

The Rayleigh scattering is measured at right angles to the focused laser beam by a monochrometer and photomultiplier, as shown in Fig. 4. As the flat plate is moved close to the beam, surface scattering will appear as a background signal and limits how close measurements can be made to the plate. In order to minimize the surface scattering, the laser beam is "cleaned up" by focussing on a pinhole, and then focussing the pinhole at the measurement volume. The waist diameter d of the focussed Gaussian mode laser beam is given by:

$$d = \frac{2\lambda}{\pi \tan \theta}$$

where θ is the included far-field angle of the converging rays[15]. Both d and θ are based on 1/e of the peak power. The waist diameter was chosen as a trade-off with several parameters. Perhaps most important, index of refraction gradients in the heated jet boundary layer

result in turbulent motion of the laser beam image of the order of 30 microns, which was determined by direct observation of the magnified image. A waist diameter of 50 microns was chosen and an ordinary two element achromat with a focal length of 126 mm was used as a focussing lens. Additional apertures were used as shown in Fig. 4 to trap light scattered from the lens surface.

An f/1.2, 55 mm focal length camera lens intended for 35 mm cameras was used to collect the scattered light. An image of the slit of the monochrometer, about 100 microns wide and 1 mm long, was focussed on the waist region of the laser beam. The optics and monochrometer (a 0.3 m McPherson) were arranged such that all the rays from the lens fell onto the photomultiplier, an RCA type 1P28, selected from several tubes for good gain and low noise. The quantum efficiency of this type of photomultiplier is about 15% at 488 nm; a more expensive tube will at best about double this value. The output current of the photomultiplier is measured using a Keithley electrometer.

A Spectraphysics argon-ion laser with nominal 1 watt power at 488 nm was used. The expected photoelectron counting rate can be estimated[14] and should be about 10^7 counts/s for air at room temperature. The observed signal-to-noise ratio is consistent with this signal level.

The most important factor in reducing background scattering from the surface of the flat plate consists of the slight bend (about 2°) down the middle of the plate, which effectively shadows the second

half of the surface of the plate from the laser beam. There is a great reduction in scattered light in this shadowed region, so that it becomes equal to the Rayleigh scattering at distances as close as 0.2 mm from the surface. A fairly sharp bend in the plate surface has been found to give the best results.

Density Gradient Visualization by Deflection Mapping

The advantage of a flow visualization method is that the entire flow field can be seen, which enables changes in the flow pattern as a function of variations in different parameters to be readily studied. The technique used in this study is a variant of the Schlieren method known as deflection mapping[13]. In both Schlieren and deflection mapping, the density gradients in the flow fields are shown On Schlieren records, the regions of maximum density gradient appear darker or lighter, depending on the type of stop used. However, a deflection mapping technique uses reference marks in the light field, so that the distribution of the density gradients can be seen as a distortion of the reference marks.

Interferometric fringes are used in the present system as the reference marks. The records thus produced have the appearance of interferograms, but the distortions of the fringes are proportional to the deflection, θ, rather than to the index of refraction, n, as in the case of interferometry. θ is defined as:

$$\theta = \int \frac{dn}{dy}\, dx$$

where n is the index of refraction, x and y are the coordinates along and normal to the optical path respectively. Since the index of refraction is linearly proportional to the density, the fringe shifts on the deflection mapping records are proportional to the density gradient in the test space provided that all other index of refraction fields along the optical path are negligible.

A schematic of the optical arrangement is shown in Fig. 5. The beam is first expanded by a short (15 mm) focal length lens, L1, then L2, a lens of f = 125 mm, is placed confocally with L1 to produce a parallel beam about 5 cm in diameter. This illuminates the test region, the center portion of the quartz plate, which is in turn imaged on a grounded glass screen, S , by lens L3. The image on the screen is observed visually and can be photographed by a 35 mm camera. The deflection mapping element is a microscope slide placed near the focus of L3 at a large inclination [16]. At such an oblique incidence, multiple reflections from the surfaces become appreciable and the reflected rays interfere to produce the fringes shown on the screen.

RESULTS AND DISCUSSION

Performance without Combustion

The velocity of the jet, without the plate, was surveyed at various axial and radial locations to determine the uniformity of the flow, the turbulence level, and the rate of growth of the jet-ambient air boundary. An example of the mean velocities and rms fluctuations, using LDV at velocities in the range of the flat plate measurements, is shown in Fig. 6. The jet velocity is quite uniform and mixing boundary layer growth is in reasonable agreement with other work[17,18]. The rms fluctuations were obtained by calculation from oscilloscope photographs of the output of the frequency tracker. The values close to the nozzle probably represent the random error in single particle tracking rather than the turbulence level in the flow, as hot wire measurements made under similar conditions indicated about 1.5% rms turbulence.

In order to understand the operation of the LDV system and the TSI Model 1090 frequency tracker more fully, accuracy tests using two trackers of the same model were carried out, and the results were compared with direct oscilliscope recordings of the LDV signal and with hot wire measurements. After proper adjustment, there was reasonably good agreement with all techniques. The hot wire indicated a turbulence level of about 1.5%, and the same value was obtained from

measurement of the Doppler burst signals. The tracker outputs indicated about 2% turbulence level. It was found that the two trackers did not always report the same velocity for each particle burst.

When a flat plate was placed in the open jet, a small degree of "blockage" of the flow was found. The free stream velocity accelerated a few percent just before reaching the plate, and this acceleration was almost uniform across the jet. Downstream of the leading edge the free stream velocity was nearly constant at the increased value.

Boundary layer velocity measurements of air over an adiabatic (unheated) plate indicate good agreement with the Blasius profile[19] as shown in Fig. 7. Further indication of this agreement is shown in Fig. 8, where the variation of boundary layer thickness with distance from the leading edge is compared with the Blasius solution.

When the plate surface is heated a numerical boundary layer solution is required in order to take into account the variable viscosity, heat conductivity, and Prandtl number of air. These computations are described in the companion paper[10]. In Fig. 7 the non-dimensional velocity is plotted as a function of distance above the plate for distances of $\hat{x}$ = 5mm and 20 mm downstream from the plate leading edge. The results presented are for an average plate surface temperature of 1180°K. Due to the variation in convective heat transfer

coefficient along the plate it was difficult to maintain a constant surface temperature up to the leading edge. The plate surface brightness temperature was measured using an optical pyrometer and it was found that the surface temperature varied from 1080°K at the leading edge to 1180°K at a distance of 2 mm downstream of the leading edge, using an estimated emissivity of 0.45. Thereafter the surface temperature remained constant at 1180 ± 10°K. The experimentally measured plate temperature profile was used as input to the computer program to obtain the present results. As shown in Fig. 9 agreement between experimental and predicted velocity profiles is within 3%. Considering uncertainties in the experimental data such agreement is considered quite good. In Figure 8 the heated boundary layer thickness is shown as a function of distance from the leading edge again indicating good agreement with the numerical computations.

Rayleigh scattering density measurements in the boundary layer were used to calculate the temperature, and the resulting profiles are shown in Fig. 10 for distances of 5 mm and 20 mm downstream. These results are corrected for background surface scattering, which contributes about 10% of the signal at 0.5 mm from the surface. The temperature (or density) profile is quite sensitive to the surface temperature, as shown in Fig. 10 by comparison with computed profiles assuming surface temperatures of 1200 K and 1250 K. Better agreement is obtained with the lower temperature. This temperature is consistent with the optical pyrometer measurement if an emissivity of 0.75 rather than 0.45 is

assumed. It should be noted that the velocity profiles are not so sensitive to the surface temperature, so that the general good agreement shown in Figs. 8 and 9 is relatively unaffected by this difference in temperature. In Fig. 11 measured and predicted thermal boundary layer thickness are shown as a function of distance along the plate. The boundary layer thickness was defined as the point at which $T/T_\infty = 2$. Good agreement is obtained if the plate temperature is taken to be 1200 K.

From the measurements and comparison with theory we conclude that the flow over the flat plate is a good approximation to idealized flat plate flow, that the laser Doppler velocimeter measurements are satisfactory, and that the measurement of density by Rayleigh scattering is a viable technique capable of accurate results.

Motion of Particles in a Temperature Gradient

When the plate was heated, the 2.0μ diameter particles added to the flow for the LDV measurements apparently move away from the surface of the plate, so that no velocity measurements could be made in the half of the boundary layer next to the plate, as will be noted in Fig. 9. Such a disappearance of particles near the plate surface was not noted with the adiabatic plate, as seen in Fig. 7, which indicates that heating of the plate causes the particles to move away from the surface.

A series of tests were made to determine the nature of the particle disappearance. The observed particle count rate as a function of distance above the plate surface is shown in Fig. 12. The expected decrease in particle count rate due to the variation in velocity and density across the boundary layer is also shown on the figure by the normalized density velocity product, $\rho\mu/(\rho\mu)_\infty$. It can be seen that the observed particle count becomes increasingly larger than expected as the edge of the dark boundary layer is approached but decreases to zero quite abruptly at a point approximately half way through the hydrodynamic boundary layer, providing a well defined boundary to the particle-free region (dark boundary layer) near the plate surface. Such behavior is consistent with the presence of some additional force acting on the particles near the plate so as to move the particles outward into the boundary layer.

A comparison of the hydrodynamic and dark boundary layer thickness is shown in Fig. 13. The dark boundary layer thickness appears to scale with the hydrodynamic boundary layer thickness. Similar results were obtained over a range of temperatures from 670 K to 1280 K and at velocities of 1.20 and 2.62 m/s.

One possible explanation for the observed particle disappearance that is consistent with the above observations is a phenomenon known as thermophoresis. It is a relatively well understood phenomenon of which considerable study has been made in the aerosol and particulate

research literature. Thermophoresis is the result of radiometric forces exerted by a gas on a nonuniformly heated object which it surrounds[20,21]. Under such conditions a flow is induced along the surface in the direction of increasing temperature due to a temperature gradient along the surface of the object. This gas flow, known as thermal creep, exerts an equal but opposite force on the surface in the direction of decreasing temperatures. For the case of a sphere in which the diameter is much greater than the mean free path, the thermophoresis force is given by:[22]

$$F_t = - \frac{6\pi M g D_p k_g \sigma}{P(2k_g + k_p)} \frac{\partial T}{\partial x} \qquad (1)$$

where D_p is the particle diameter, k is the thermal conductivity, μ is the viscosity, P is the gas pressure, and σ is the thermal slip factor ($\sigma = 0.2$). Thus, the thermophoresis force is linearly proportional to the local temperature gradient and in the direction of decreasing temperature.

The computer program was modified to calculate particle trajectories during flow over the heated plate. A Lagrangian coordinate system was used in which particle motion was determined by the effects of Stokes drag and the thermophoresis force given by Eq. (1).

Initial calculations indicate that the resulting thermophoresis force as predicted by Eq. (1) are about an order of magnitude less

than that required to account for the observed behavior. It should be noted, however, that these results are very preliminary and subsequent calculations are currently being continued.

Boundary Layer Combustion

Most measurements to date have been made with lean hydrogen-air mixtures, generally below the flammability limit at standard temperature and pressure. This ensures that combustion will take place only within the heated boundary layer. Also, envisioned practical applications of catalyzed combustion are generally with quite lean mixtures. The present work is in a preliminary stage, and there has been difficulty in obtaining satisfactory quartz flat plates with a long life. Measurements have been made on three different plates, and the results will be described in chronological order.

On the first plate tested the platinum heating strips were overcoated with silicon monoxide, a standard coating used to protect aluminum mirrors and which we expected to be "non-catalytic". This coating may have oxidized to silicon dioxide (quartz) during the tests. It was necessary to have a surface temperature of about 1300 K before faint visible emission from combustion reactions could be seen in the boundary layer.

Only velocity profile measurements were made with this plate, as the platinum heating strips burned out during Rayleigh scattering density measurements. The velocity profiles were similar to those measured

without fuel. In Fig. 14 the boundary layer thickness is compared with the numerical computations for a non-catalytic surface. In these computations the actual wall temperature, which varied with distance downstream and is shown in Fig. 15, was used. The computations predict the onset of combustion at 2 mm downstream, where the boundary layer velocity thickness is increased by more than 50% due to the rapid heat release during combustion. However, the surface temperature as shown in Fig. 15 shows a sharp increase at 7 mm, indicating that the actual onset of combustion with the attendant change in heat transfer occurred at this distance. Also shown on the figure is the numerical solution without any combustion, but with all other conditions identical. The measured boundary layer thicknesses lie between the two cases, and significantly closer to the combustion case. (Compare with the agreement shown in Fig. 8 for the test case without combustion). Our tentative conclusion is that the onset of combustion actually occurred at 9 mm, and that the reaction rates used in the computations are too high.

Figure 14 also shows the numerical results for the thermal boundary layer thickness, with and without combustion. There is a much larger predicted increase in thermal thickness associated with combustion than with the velocity thickness. This information will be used in drawing a conclusion from the Rayleigh scattering measurements to be described next.

This plate was recoated and covered with a silicon dioxide (quartz) surface, about 0.1 micron thick, for the next measurements. Because of coating difficulties, only the first three strips, covering 25 mm downstream, were useable. Only Rayleigh scattering density measurements were made with this plate, at surface temperatures of 1250 K, a little lower than with the first plate, and 1100 K. The density profiles appeared very similar to those measured without hydrogen, as shown in Fig. 10, and extrapolated to a surface temperature close to that determined by the optical pyrometer. A summary of the boundary layer thicknesses obtained from the detailed profiles is shown in Fig. 16, with equivalence ratios of 0, 0.05, and 0.1, and are compared with the numerical solution for no combustion. These results indicate that no combustion occurred at this temperature, since there is not a consistent trend in the measurements at different equivalence ratios, and there is reasonable agreement with the solution for no combustion. Further, a numerical solution for the case with combustion, as shown in Fig. 14 for slightly lower wall temperature, predicts a very large increase in thermal boundary layer thickness.

For the silicon monoxide coated plate we concluded that combustion occurred at 9 mm, and was initiated with a wall temperature of 1100 K as shown in Fig. 15. For the silicon dioxide coated plate there was no combustion, and the wall temperature was nearly constant at 1250 K, except near the leading edge. Our present conclusion is that the catalytic surface activity of the silicon monoxide plate helped initiate

combustion, and that the silicon dioxide coated plate had significantly less catalytic activity. Since the reactions and rate constants used in the numerical computations, performed for a non-catalytic surface, predict very rapid ignition at 1250 K, it is obvious that these rates are considerably too large.

The third plate tested had a bare platinum surface, with no over-coating. After unsuccessful trials with a second quartz plate, with a polished surface to which the platinum would not adhere satisfactorily, the plate used in the first two measurements was recoated. It was used without problems until it cracked down the middle during the measurements, the first failure of a quartz plate substrate.

The deflection mapping technique was used to take photographs of the density gradient in the boundary layer, and examples are shown in Figs. 17-20. These photographs, and visual study of the patterns for different parameters, were of considerable aid in understanding some of the phenomena which occurred. Figure 17 shows the boundary layer density profile with no fuel in the flow and a surface temperature of 1080 K. The point of maximum deflection of the fringes represents the largest density gradient, which occurs at a temperature rise of about 140 C for a wall temperature of 1080 K.

Figure 18 shows the same surface temperature and flow rate, but with hydrogen fuel at an equivalence ratio equal to 0.1. The boundary layer is considerably thicker, which indicates that the effect of

surface catalysis involves more than simply the generation of combustion reactions at the surface. In that case the boundary layer temperature profile and thickness would hardly be changed, and the only effect would be to reduce the electrical power required to maintain the surface at 1080 K. In order to have a thicker boundary layer with the same surface temperature, homogeneous combustion with significant heat release must have taken place in the boundary layer. Since the data taken with the silicon dioxide coated plate indicated that no combustion occurred with wall temperatures up to 1250 K, it appears that chain carriers of some sort are generated at the platinum surface, diffuse into the boundary layer, and speed up the combustion reactions.

In Fig. 19 the heating power to the first platinum strip has been turned off; however, a thermal boundary layer is being generated beginning at the leading edge (with no fuel present the thermal boundary layer starts at the second strip). The temperature of this first strip under these conditions is unknown, but less than 900 K, the lower limit of the optical pyrometer. Beginning with the second strip, which was maintained at 1080 K, the boundary layer begins to grow more rapidly in thickness. Apparently streamwise heat conduction, either in the boundary layer or in the quartz plate substrate, is sufficient to raise the surface temperature high enough to initiate combustion heat release. This is borne out by experiments in which only the third strip was slowly heated, while watching the deflection mapping image on a screen. Initially there was a thermal boundary layer beginning at the third strip,

but then this thermal boundary lyaer would advance slowly forward right to the leading edge of the plate.

In Fig. 20 combustion is maintained over the plate without any electrical heating power. In this particular example, with $\phi = 0.2$, there were two zones of combustion; an initial zone extending from the leading edge to about 1 cm downstream where the surface temperature was less than 1000 K, and then a sharp rise in surface temperature to 1200 K or more. In the figure this transition is indicated by a more rapid growth of the boundary layer. One explanation is that ignition of the homogeneous reactions begins at this point.

Rayleigh scattering density profiles have been taken over this plate, but the data have not yet been analyzed.

The change in heat transfer at the plate surface due to combustion was obtained by measuring the electrical power input to each heating strip as a function of fuel equivalence ratio, while holding the surface temperature constant. This gives the average change in heat transfer over the area of the strip, including surface catalyzed reactions and conductive heat transfer into the boundary layer. Figure 21 shows the heating powers for the four strips, with no fuel, and the decrease in heating power at equivalence ratios of 0.1, 0.2, and 0.3. No electrical heating power was necessary for the first strip with $\phi = 0.3$. Comparison with numerical calculations are planned.

Measurements were also made with methane as fuel. Photographs and observations of the deflection mapping technique indicated very little, if any, heat release from combustion reactions at surface temperatures up to 1300 K. Also, surface heat transfer measurements did not indicate any significant change at different methane equivalence ratios. As is well known, methane is difficult to ignite, but it was surprising that a platinum surface at 1300 K would not initiate a significant amount of combustion.

SUMMARY

A facility for studying combustion in the boundary layer of a heated flat plate has been constructed and tested. The principal diagnostic techniques consist of laser Doppler velocimetry for measurement of boundary layer velocity and Rayleigh scattering for measurement of boundary layer density. Relative heat transfer measurements and deflection mapping images of the flow field have also been made. Verification of the flow and diagnostic techniques has been carried out using pure air flows. Measurements with a silicon dioxide "non-catalytic" surface indicate no combustion of a lean hydrogen-air mixture at surface temperatures up to 1200 K. Measurements with a platinum catalytic surface and lean hydrogen-air mixtures indicate significant surface combustion at temperatures less than 900 K. At a temperature of 1000 K thickening of the boundary layer indicates that significant gas phase combustion is induced by the presence of the catalytic surface, presumably by diffusion of active species generated at the surface into the boundary layer.

REFERENCES

1. D. M. Anderson, "Effects of Equivalence Ratio and Dwell Time on Exhaust Emissions from an Experimental Premixing Prevaporizing Burner," NASA TM X-71592 (1975).
2. R. W. Schefer and R. F. Sawyer, Sixteenth Symposium (International) on Combustion (to be published), The Combustion Institute, Boston, Mass (1976).
3. J. P. Kesselring, coordinator, Workshop on Catalytic Combustion, Raleigh, North Carolina, May 25-26, 1976.
4. Second Workshop on Catalytic Combustion, Raleigh, North Carolina, June 21-22, 1977. Sponsored by the U.S. Environmental Protection Agency. Summary prepared by J. P. Kesselring, Acurex Corp., Mountain View, CA (unpublished).
5. W. C. Pfetterle, R. M. Heck, R. V. Carruba, and G. W. Roberts, "Catathermal Combustion: A New Process for Low-Emission Fuel Conversion," ASME paper 75-WA/FU-1, Winter Annual Meeting, Houston, Texas, Nov. 30 - Dec. 4, 1975.
6. W. S. Blazowski and G. S. Bresowar, "Preliminary Study of the Catalytic Combustor Concept as Applied to Aircraft Gas Turbines," AFAPL-TR-74-32, Wright-Patterson Air Force Base, May 1974.
7. R. M. Heck, presentation at the Second Workshop on Catalytic Combustion, Raleigh, North Carolina, June 21-22, 1977. (see ref. 4)

8. J. P. Kesselring, W. V. Krill and R. M. Kendall, "Design Criteria for Stationary Source Catalytic Combustors", presented at the Second Workshop on Catalytic Combustion, Raleigh, North Carolina, June 21-22, 1977. (see ref. 4)

9. J. P. Kesslering, R. A. Brown, R. J. Schreiber, and C. B. Moyer, "Catalytic Oxidation of Fuels for NO_x Control from Area Sources," EPA Report EPA-600/2-76-037 (February 1976).

10. R. Schefer and F. Robben, "Catalyzed Combustion in a Flat Plate Boundary Layer. II. Numerical Calculations," to be presented at the Western States Section, The Combustion Institute, Oct. 17-18, Stanford, CA.

11. S. A. Self and J. H. Whitelaw, "Laser Anemometry for Combustion Research," Combustion Science and Technology 13, p. 171-198 (1976).

12. F. A. Jenkins and H. E. White, Fundamentals of Optics, McGraw-Hill, New York, 1957, p. 462.

13. F. J. Weinberg, Optics of Flames, Butterworths, London, 1963.

14. F. Robben, "Comparison of Density and Temperature Measurement Using Raman Scattering and Rayleigh Scattering," Combustion Measurements: Modern Technique and Instrumentation, edited by R. Goulard, pp. 180-196, Hemisphere Publishing Corp., Washington, DC, 1976.

15. A. Yariv, Introduction to Optical Electronics, Holt, Rinehart and Winston, New York, 1971, p. 35.

16. A. K. Oppenheim, P. A. Urtiew and F. J. Weinberg, "On the Use of Laser Light Systems in Schlieren - Interferometer Systems," Proc. Roy. Soc. A291, p. 279-290 (1966).

17. N.W.M. Ko and A.S.H. Kwan, J. Fluid. Mech. 73, part 2, p.305 (1976).

18. G. D. Catalano, J. B. Morton and R. R. Humphris, AIAA Journal 14, No. 9, p.1157 (1976).

19. H. Schlicting, Boundary Layer Theory, 6th Ed., McGraw-Hill, New York, 1968.

20. N. A. Fuchs, The Mechanics of Aerosols, p. 66, Pergamon Press, New York (1964).

21. L. B. Loeb, The Kinetic Theory of Gases, p. 353, Dover Publications, New York (1961).

22. L. Waldman, Proc. Second International Symposium on Rarified Gas Dynamics (L. Talbot, ed.), Academic Press, 1961.

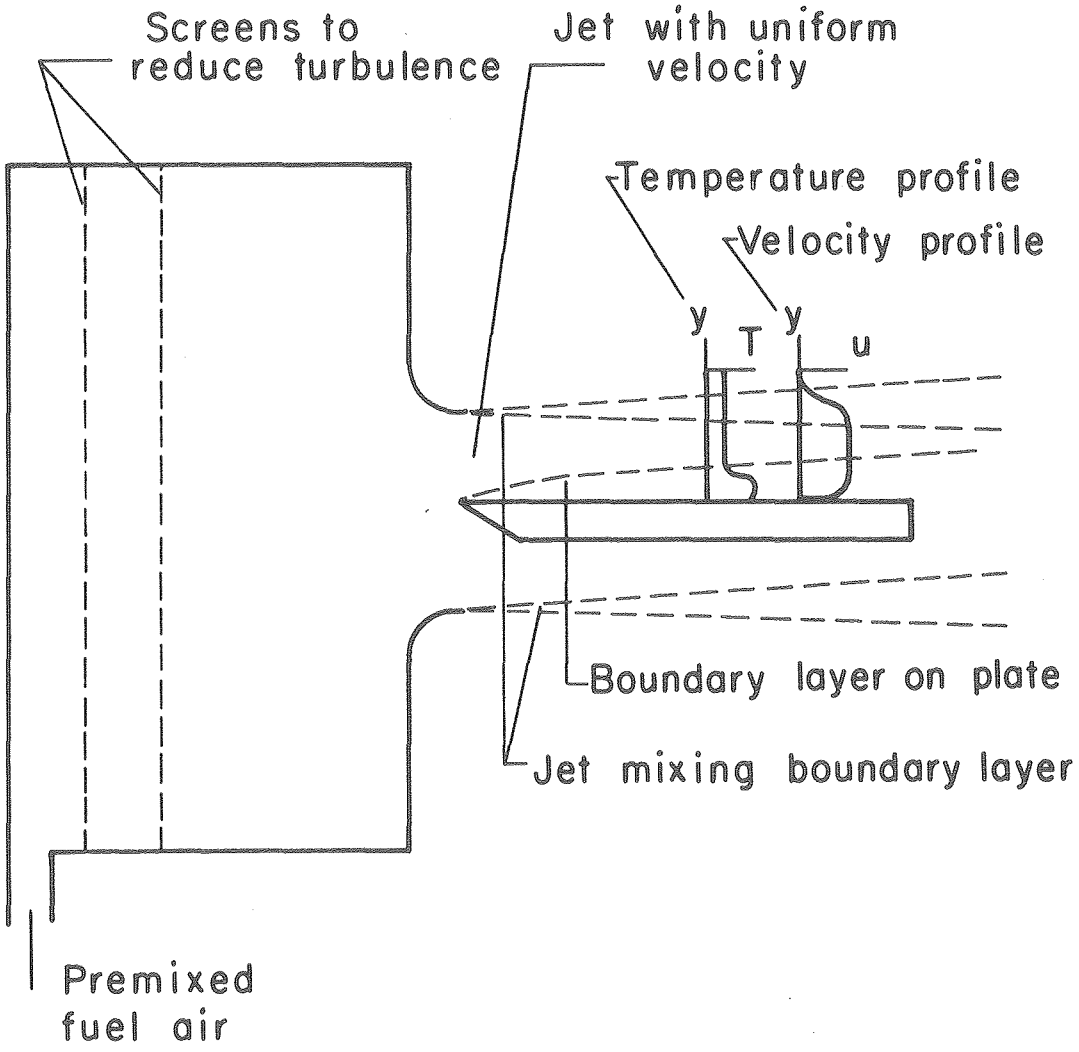

Figure 1. Schematic of the flow over a heated flat plate with combustion occurring in the boundary layer.

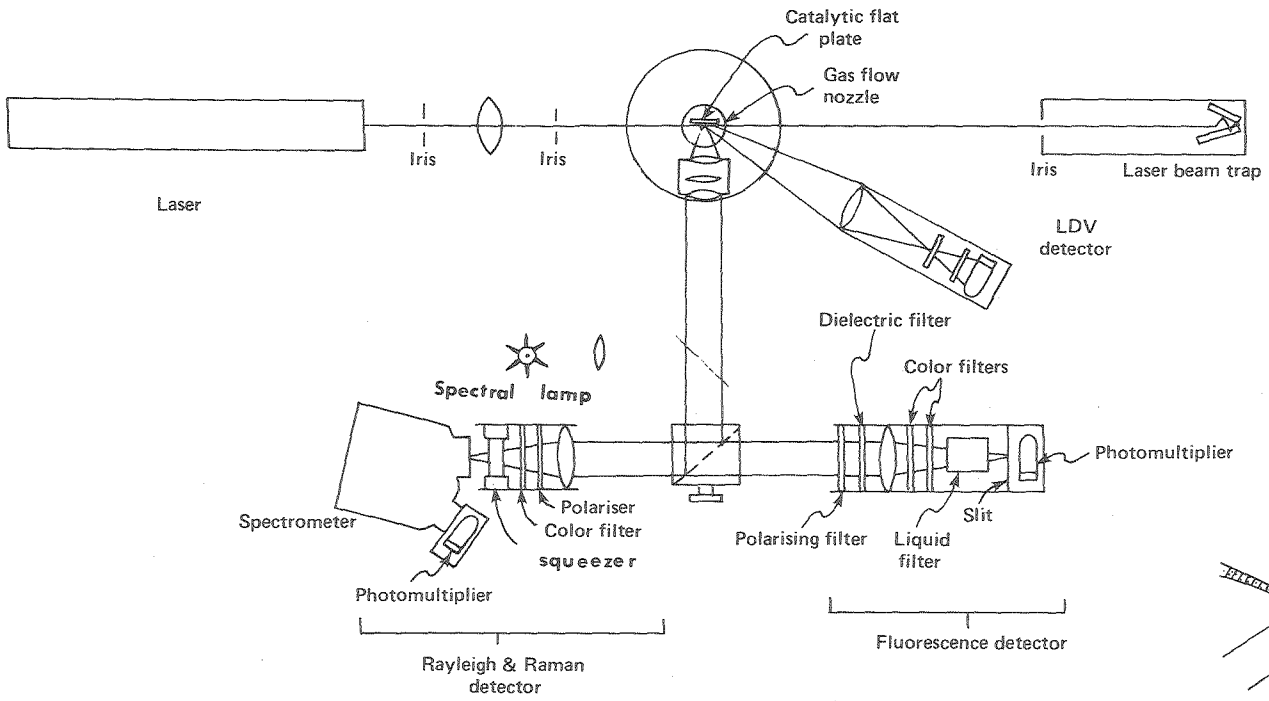

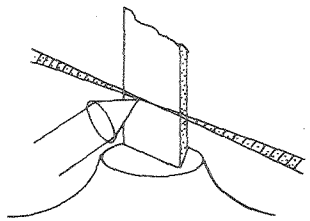

XBL 764-2757

Figure 2. Schematic of the experimental apparatus for measurement of velocity and density boundary layer profiles over a flat plate.

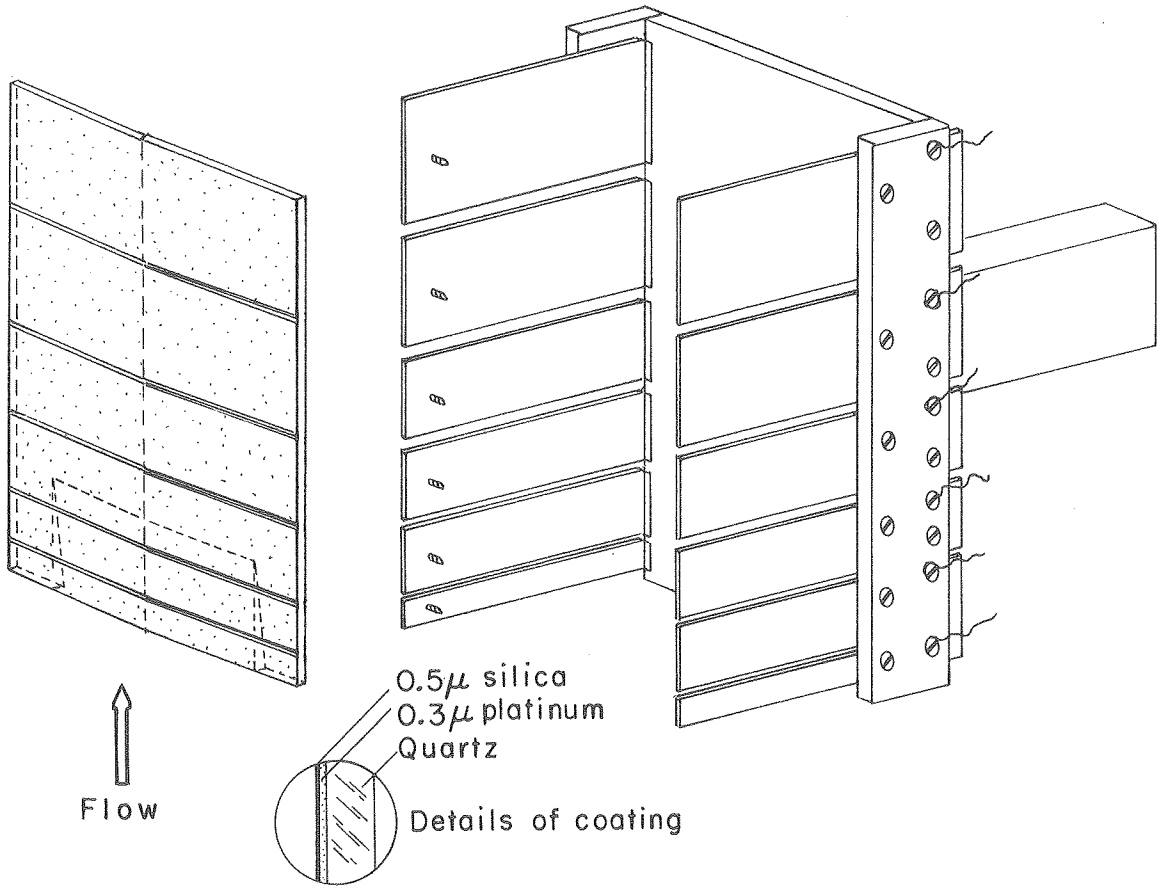

Figure 3. Design of the quartz flat plate and the holder.

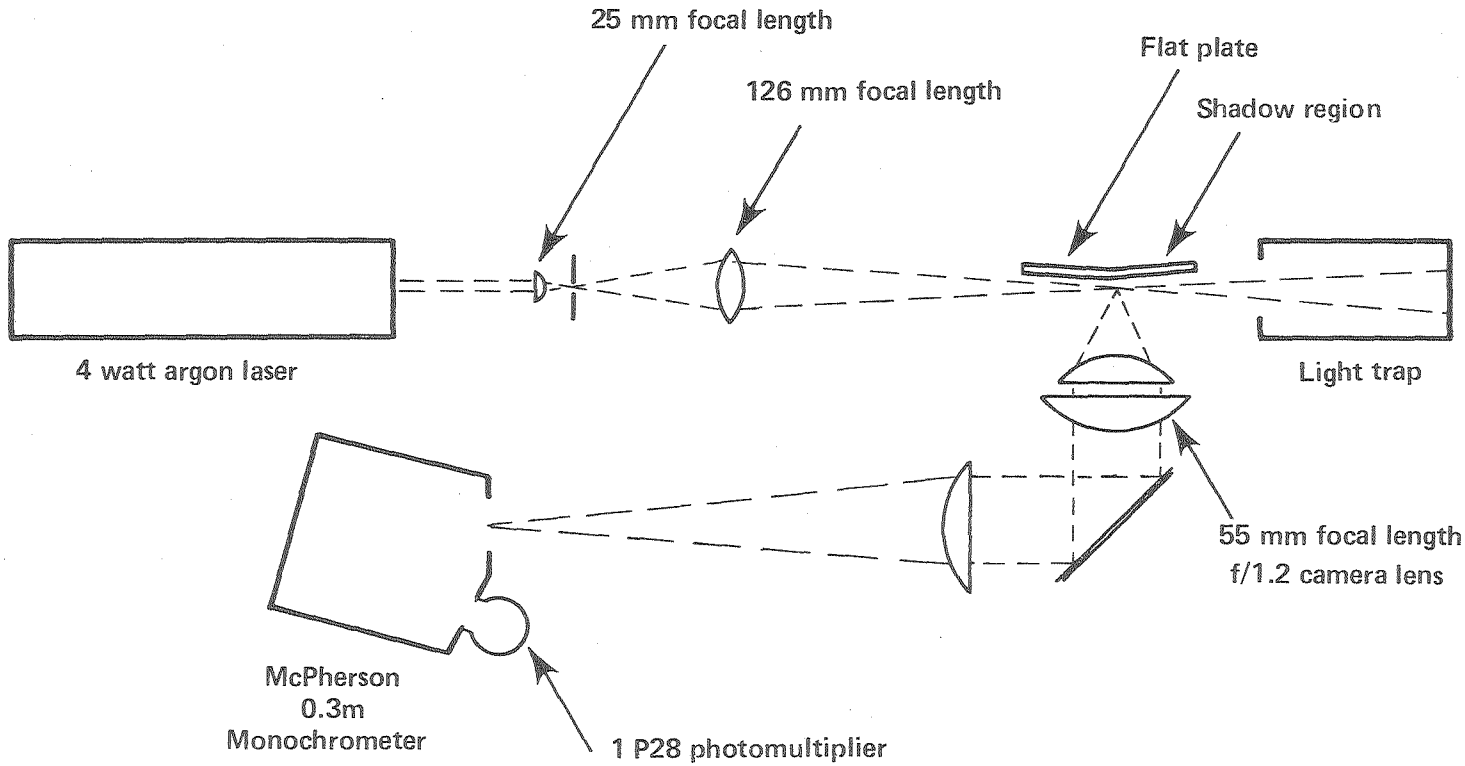

Figure 4. Schematic of the optics for Rayleigh scattering measurements.

XBL 779-1979

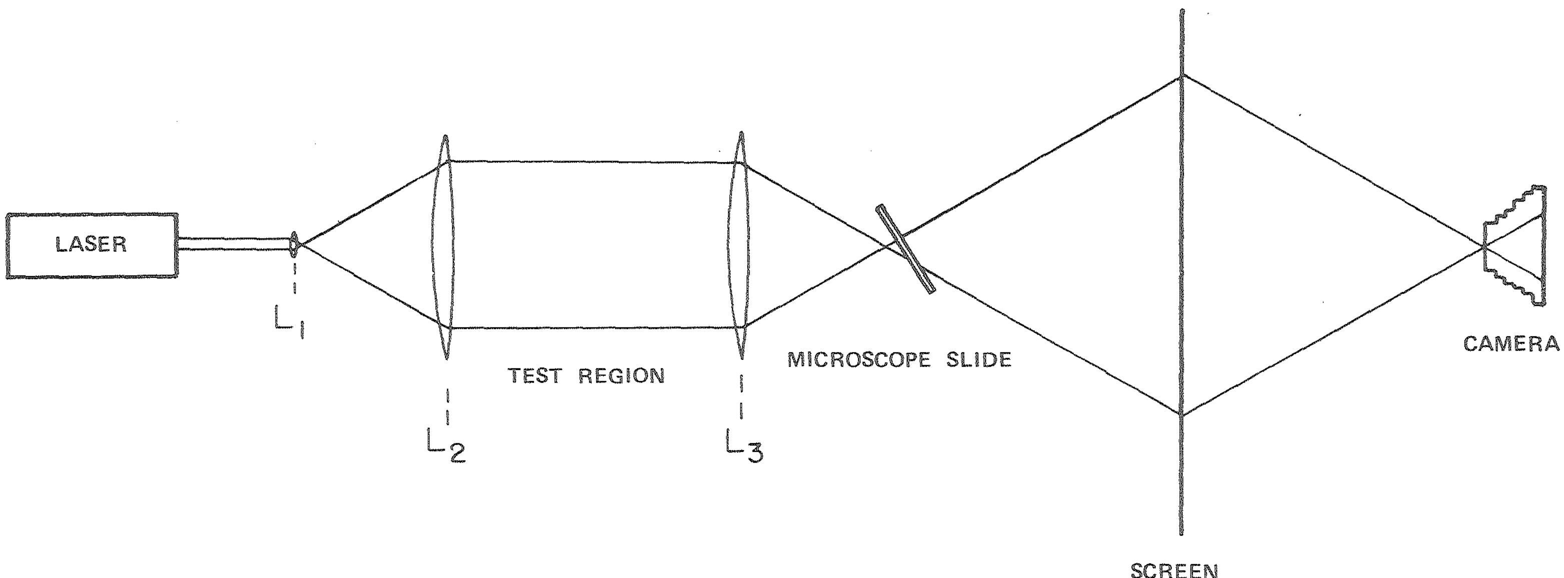

Figure 5. Schematic of the optics for deflection mapping of the density gradients in the boundary layer.

XBL 779-2014

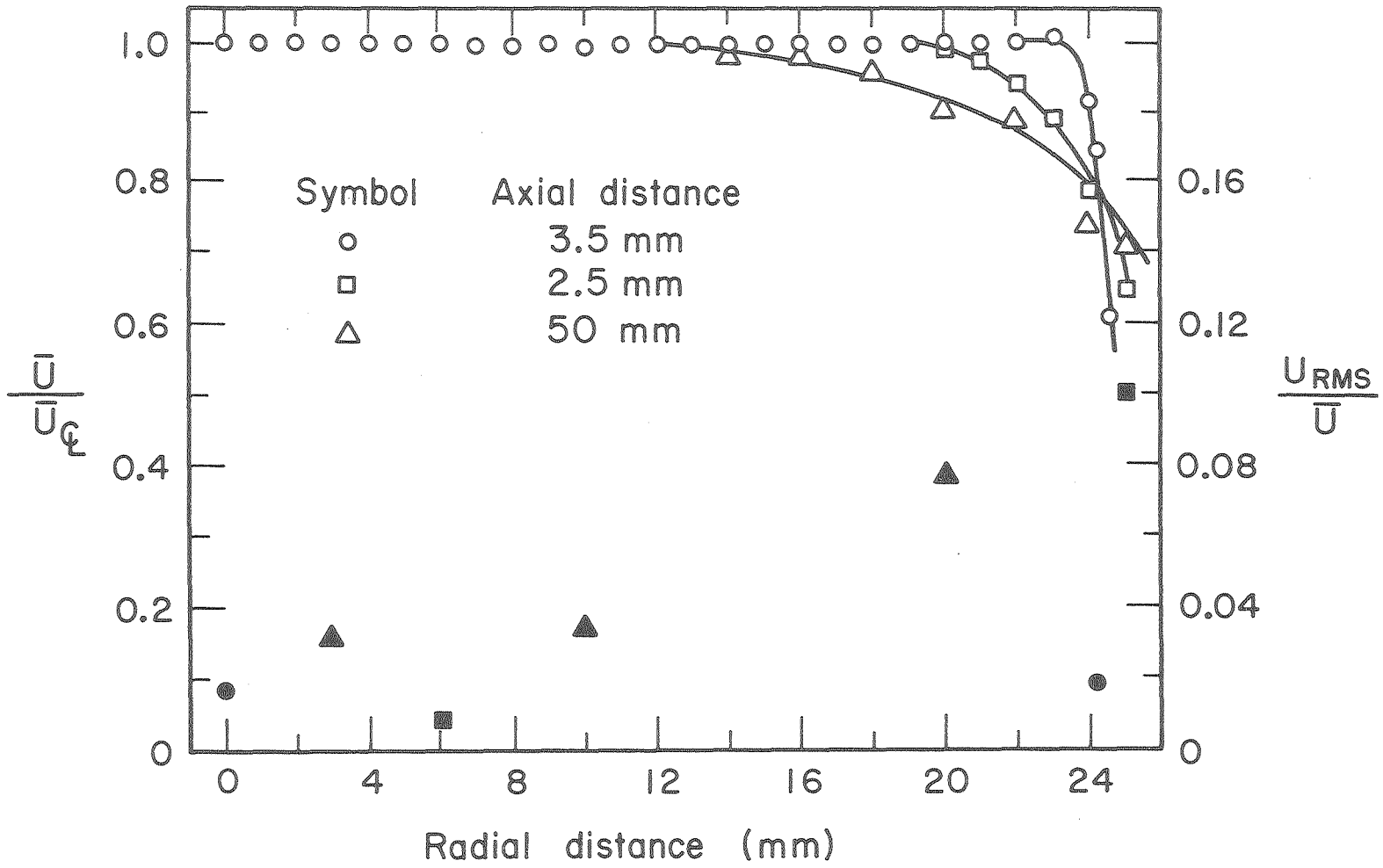

XBL 779-2001

Figure 6. Mean and RMS turbulent velocities in the jet, without the flat plate, as a function of radius and axial distance downstream from the nozzle. The open symbols are mean values, and the closed symbols are the turbulent values.

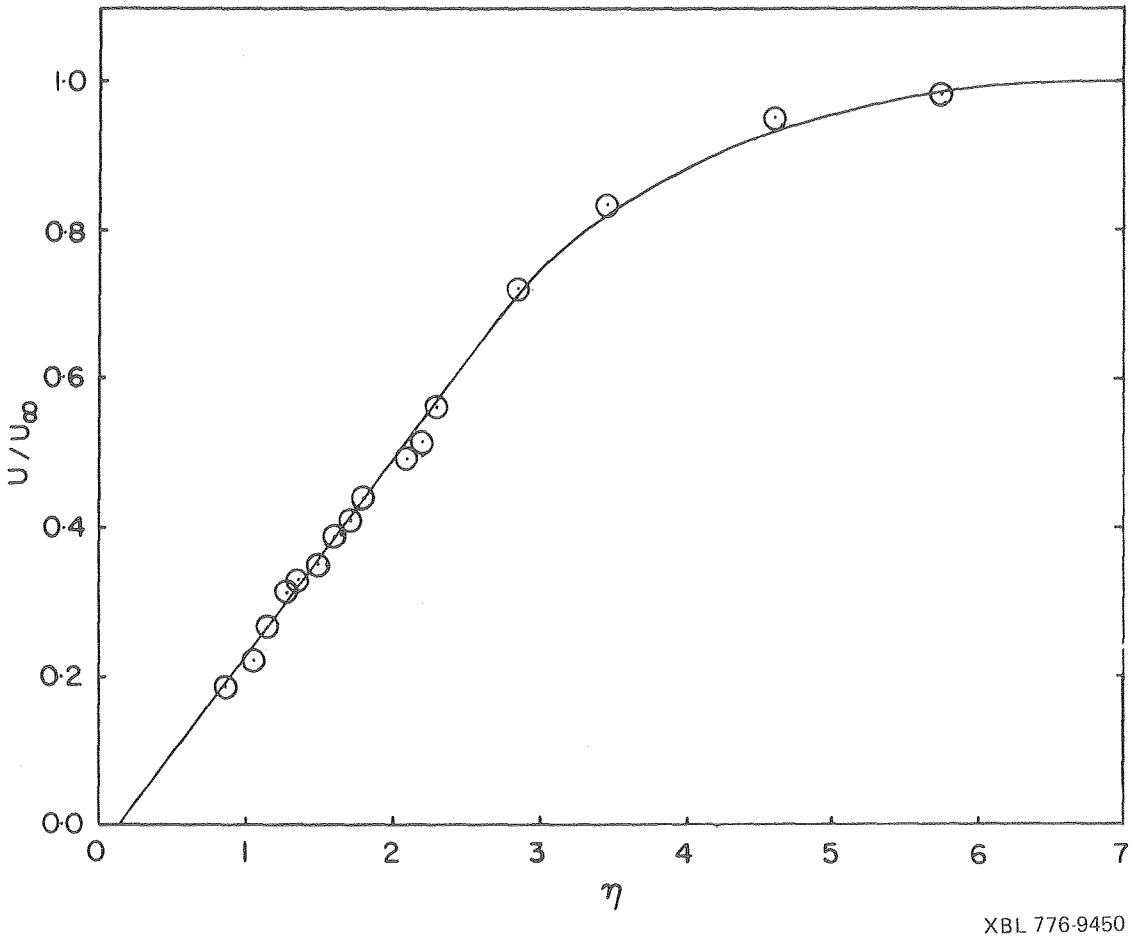

Figure 7. Comparison of the measured boundary layer velocity profile over the unheated (adiabatic) flat plate with the Blasius profile. η is the non-dimensional distance from the plate surface.

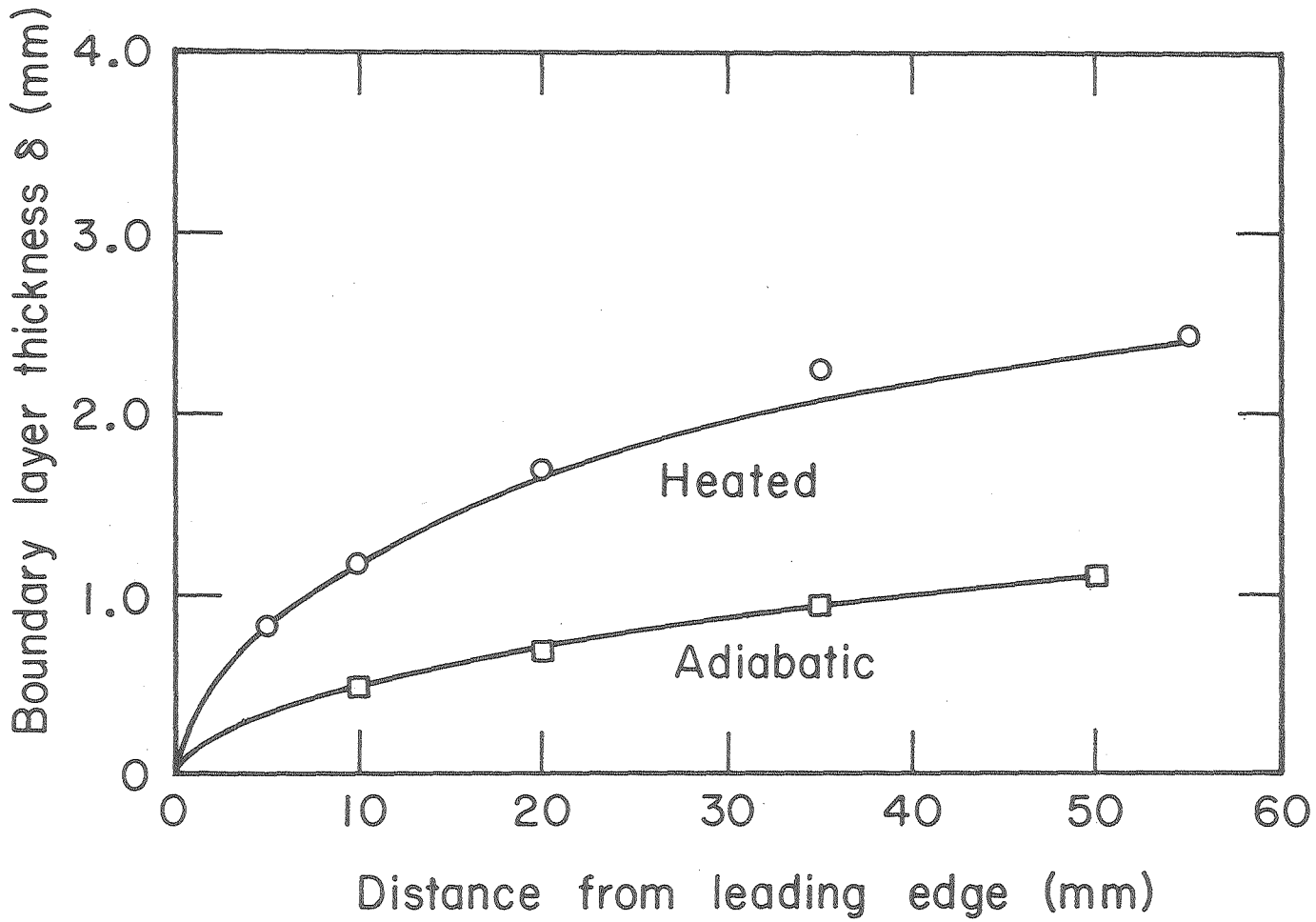

Figure 8. Comparisons of measured and calculated boundary layer thicknesses, based on $U/U_\infty = 0.7$. The free stream velocity $U_\infty = 3.17$ m/s for both the adiabatic and heated plate; the heated plate wall temperature was 1180 K.

XBL 779-1999

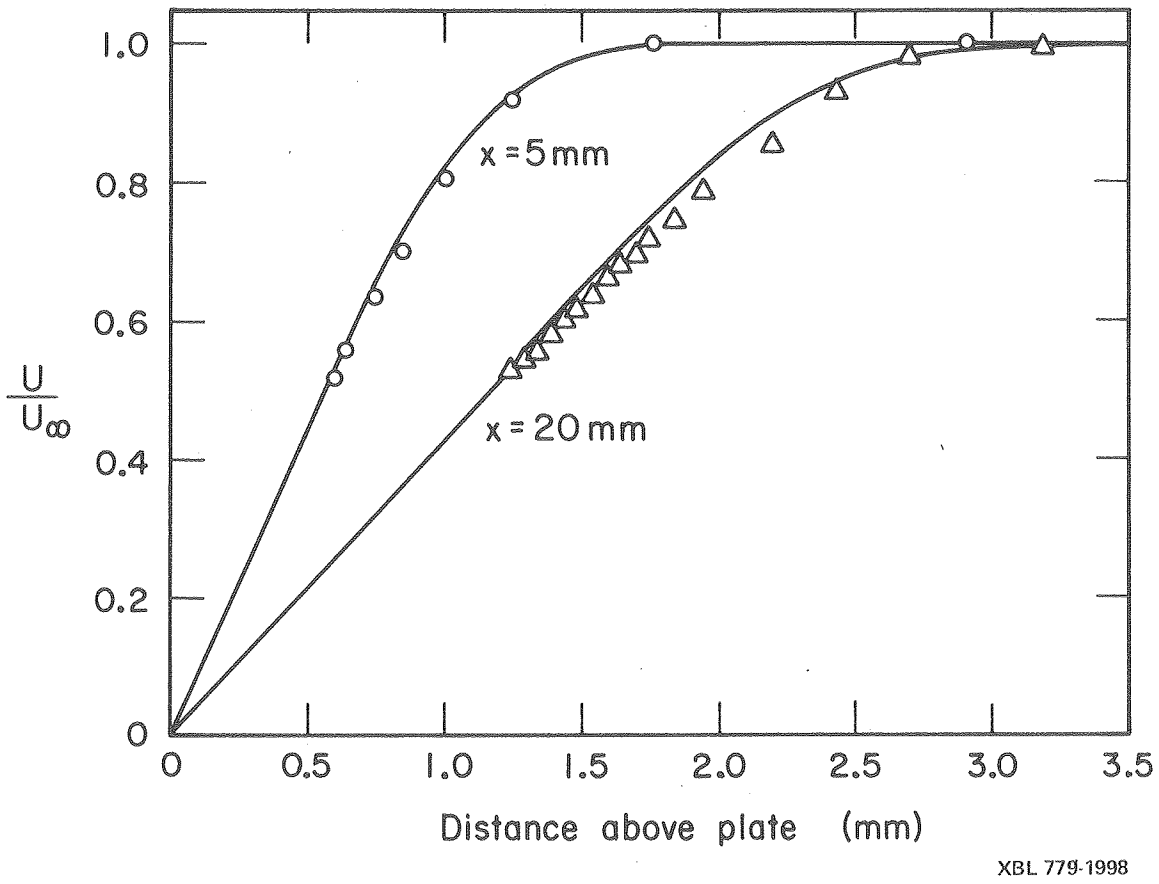

Figure 9. Comparison of measured and calculated velocity profiles over a heated flat plate, with U_∞ = 3.17 m/s and T_{wall} - 1180 K.

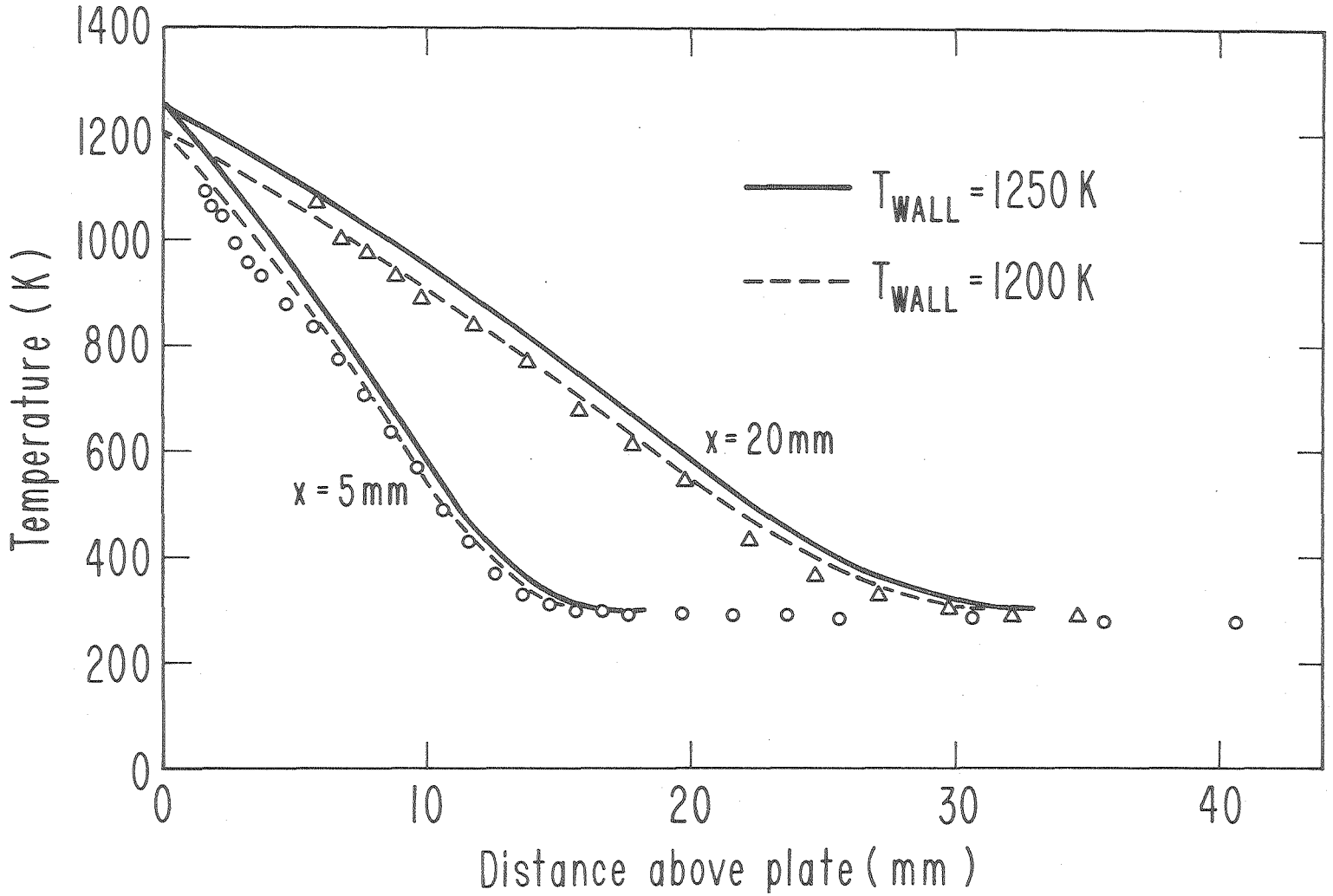

Figure 10. Comparison of measured and calculated temperature profiles over a heated flat plate, with U_∞ = 3.17 m/s.

XBL 779-1981

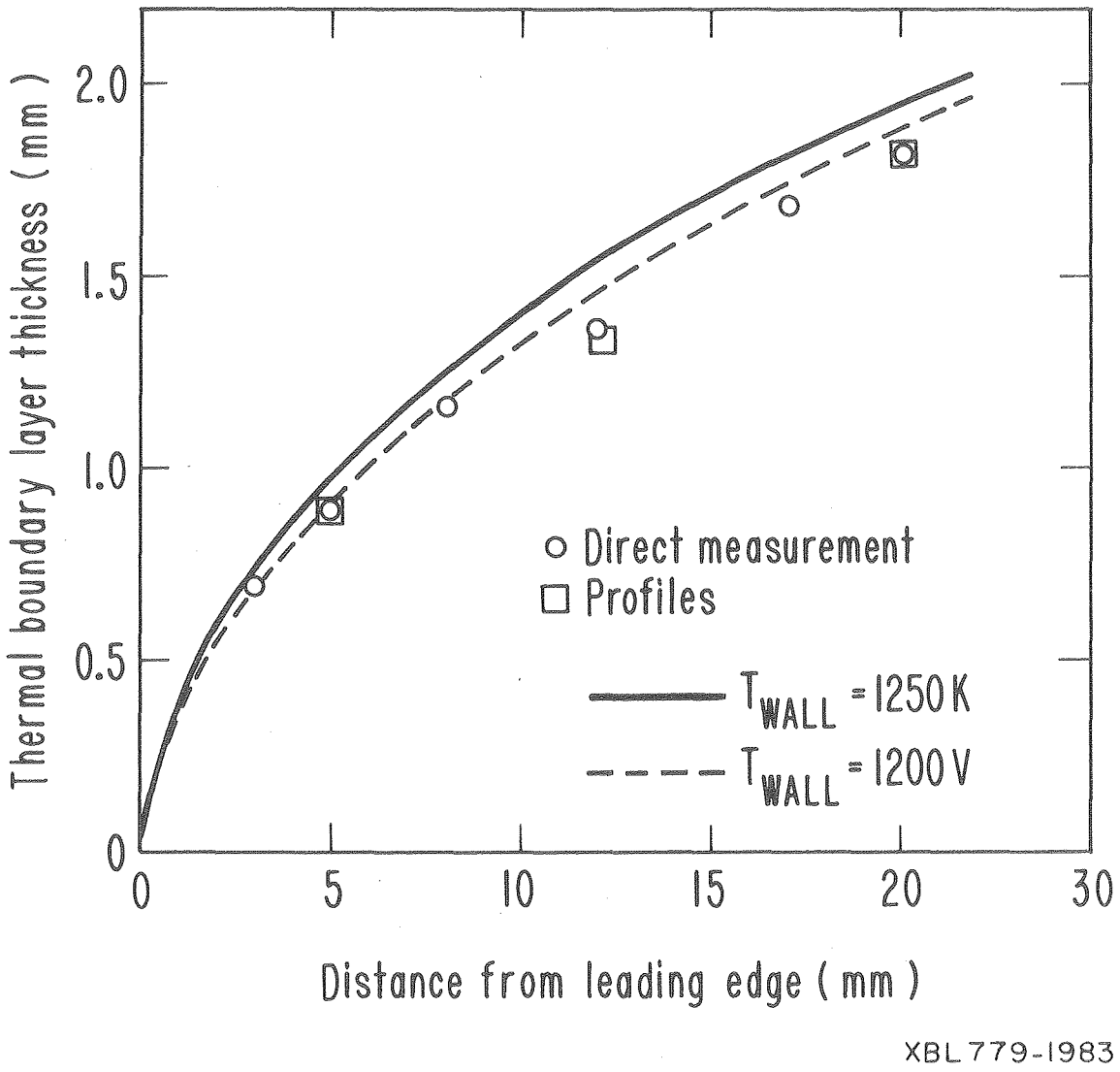

Figure 11. Comparison of measured and calculated boundary layer thickness, based on $T/T_\infty = 2.0$, with $U_\infty = 3.17$ m/s.

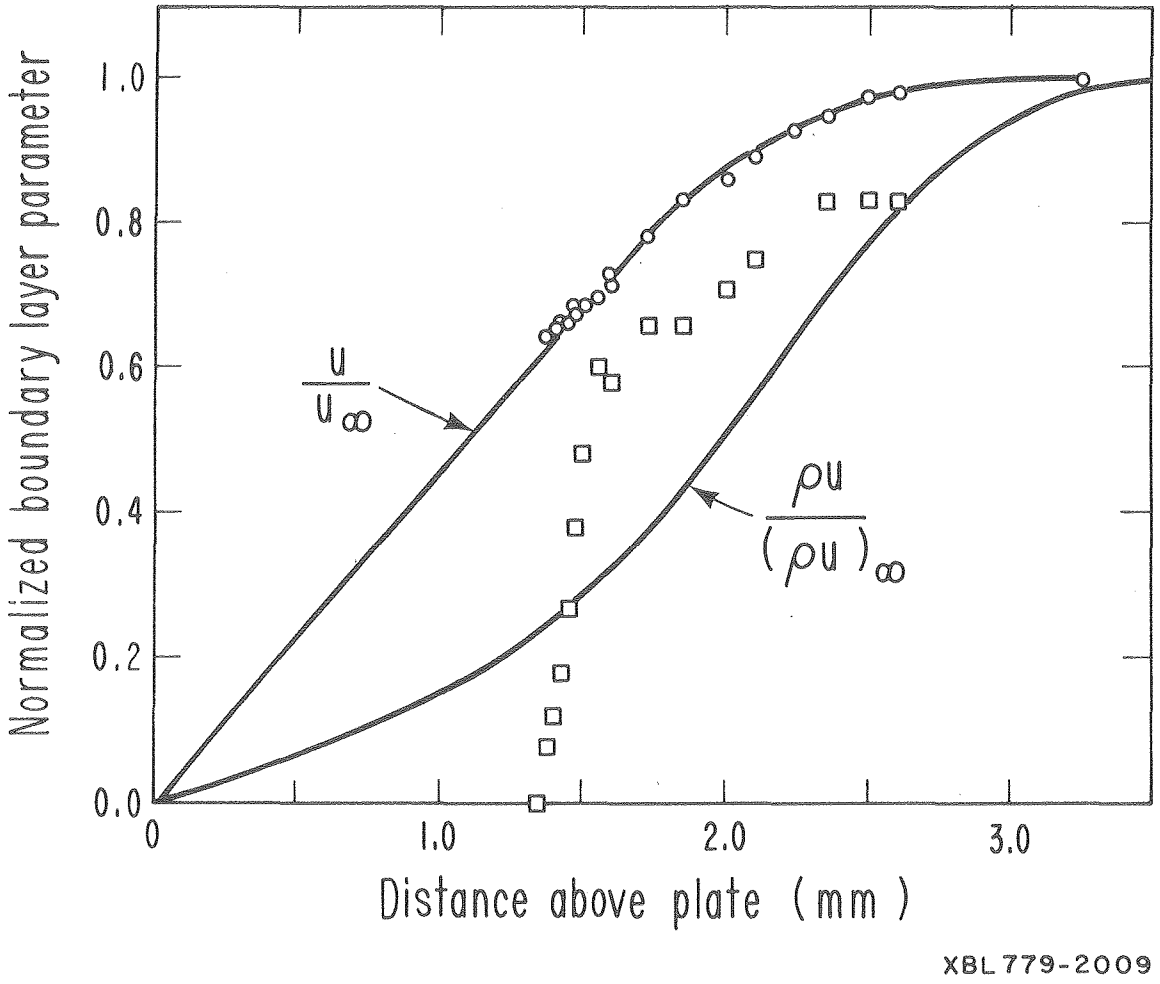

Figure 12. Comparison of measured velocity, particle count rate, and normalized density-velocity product profiles for a heated plate at 1200 K, U_∞ = 2.62 m/s. The measurements were made at 25 mm downstream from the leading edge.

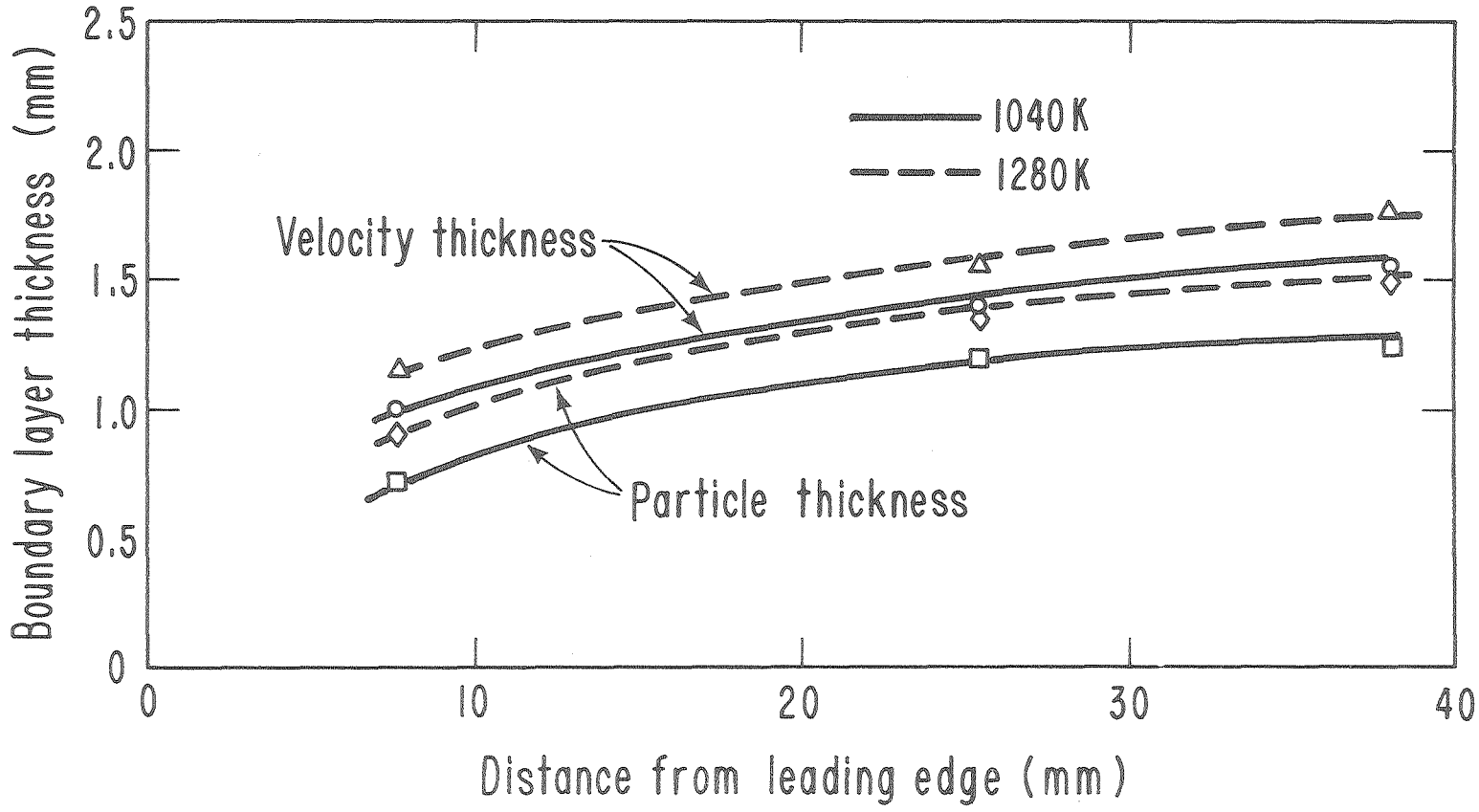

XBL779-2010

Figure 13. Comparisons of boundary layer velocity thickness (U/U_∞ = 0.7) and particle-free thickness as a function of distance downstream, for two surface temperatures with U_∞ = 2.62 m/s.

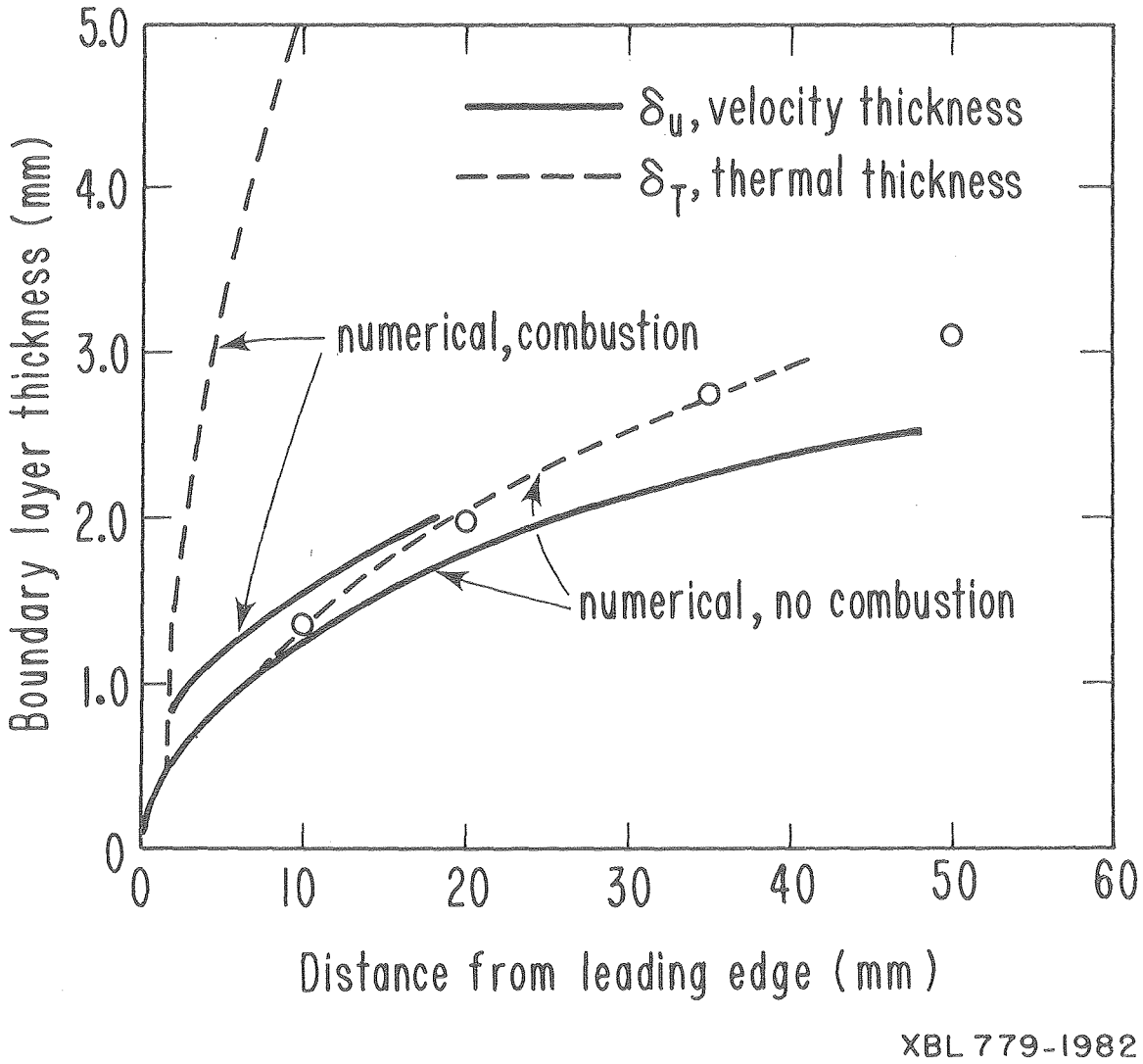

Figure 14. Comparison of measured boundary layer thickness for a 0.1 equivalence ratio hydrogen-air mixture with numerical calculations. The velocity boundary layer thickness is based on U/U_∞ = 0.7, and numerical results are shown with combustion occurring according to the assumed kinetics, and without combustion. The plate surface was coated with silicon monoxide, with nominal surface temperature of 1100 K (see Fig. 15) and U_∞ = 3.17 m/s. Also shown are numerical equations for the thermal boundary layer thickness, based on T/T_∞ = 2.0

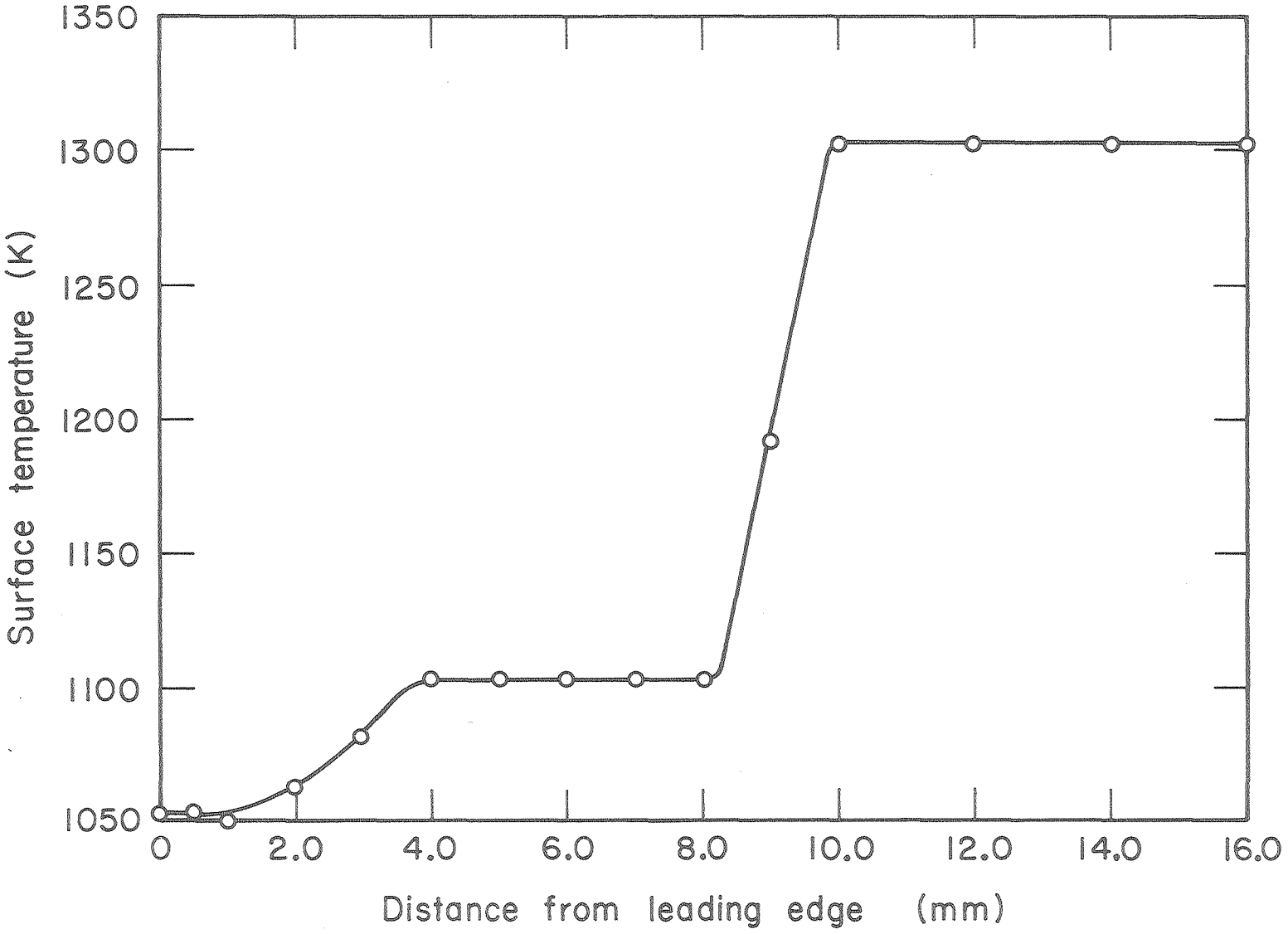

XBL 779-2000

Figure 15. Plate surface temperature as a function of distance downstream, measured by an optical pyrometer, for the data and computations shown in Fig. 14.

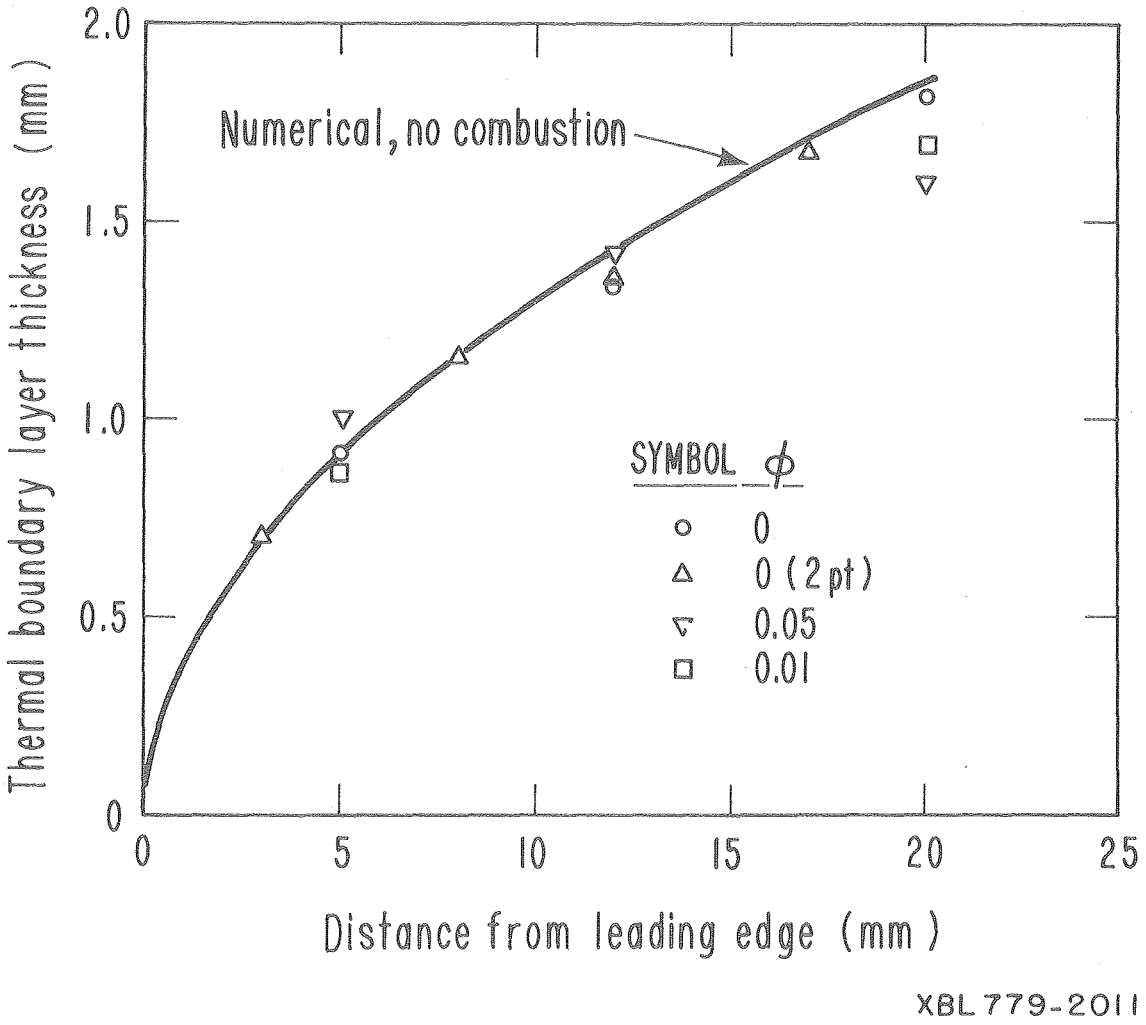

Figure 16. Comparison of measured thermal boundary layer thickness (T/T_∞ = 2.0) at hydrogen-air equivalence ratios of 0.0, 0.05, and 0.10. Silicon dioxide coated plate with surface temperature of 1250 K and free stream velocity 3.17 m/s. Also shown is the numerical result for combustion.

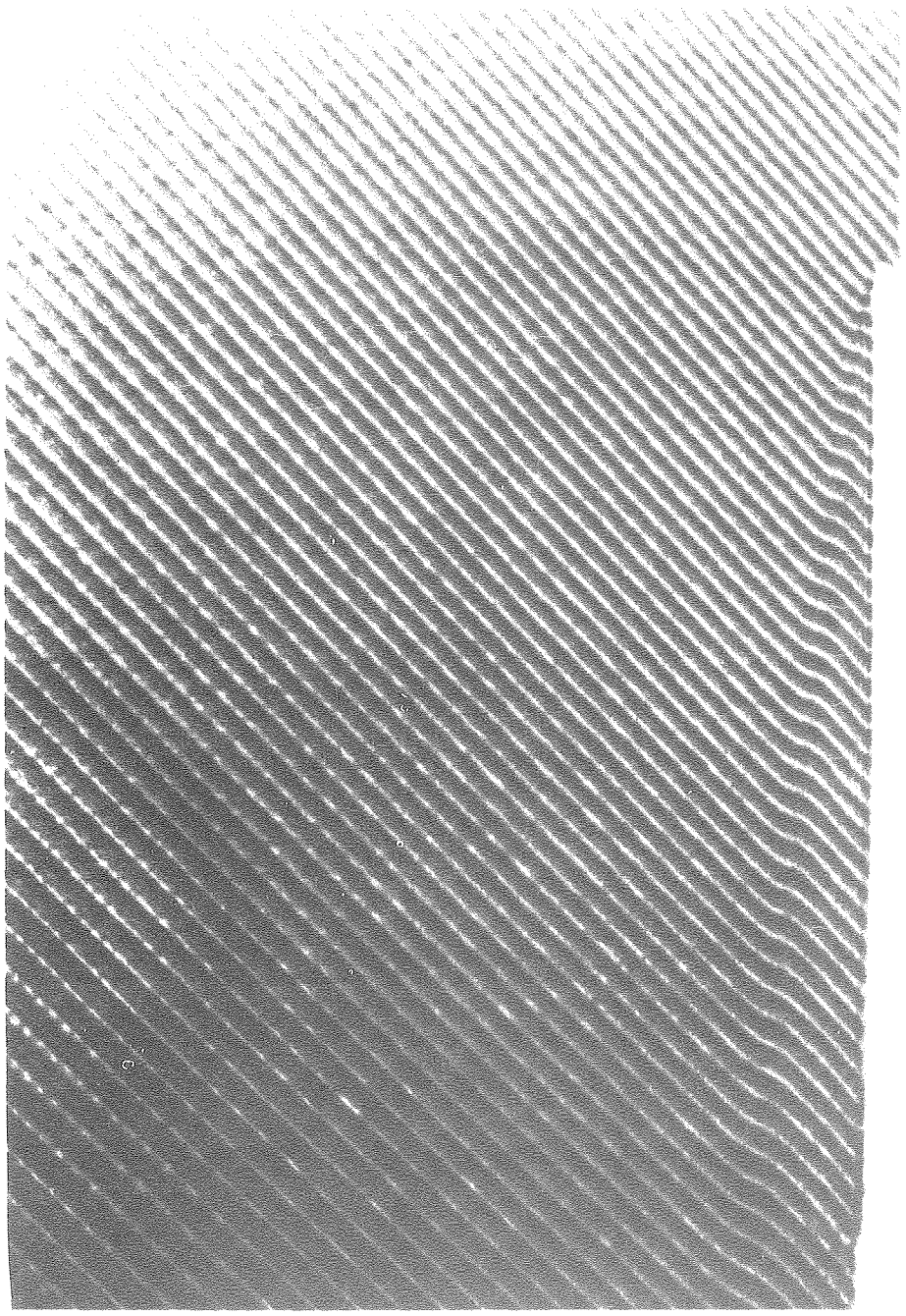

XBB 7710-9523

Figure 17. A deflection mapping photograph of the density gradient in the boundary layer over the heated flat plate. The leading edge is at the top of the figure, and the density gradient is proportional to the deflection of the fringe from the straight line extrapolation outside the boundary layer. This photograph is for the flow of air over the platinum coated plate, with uniform surface temperature of 1080 K and free stream velocity of 3.17 m/s.

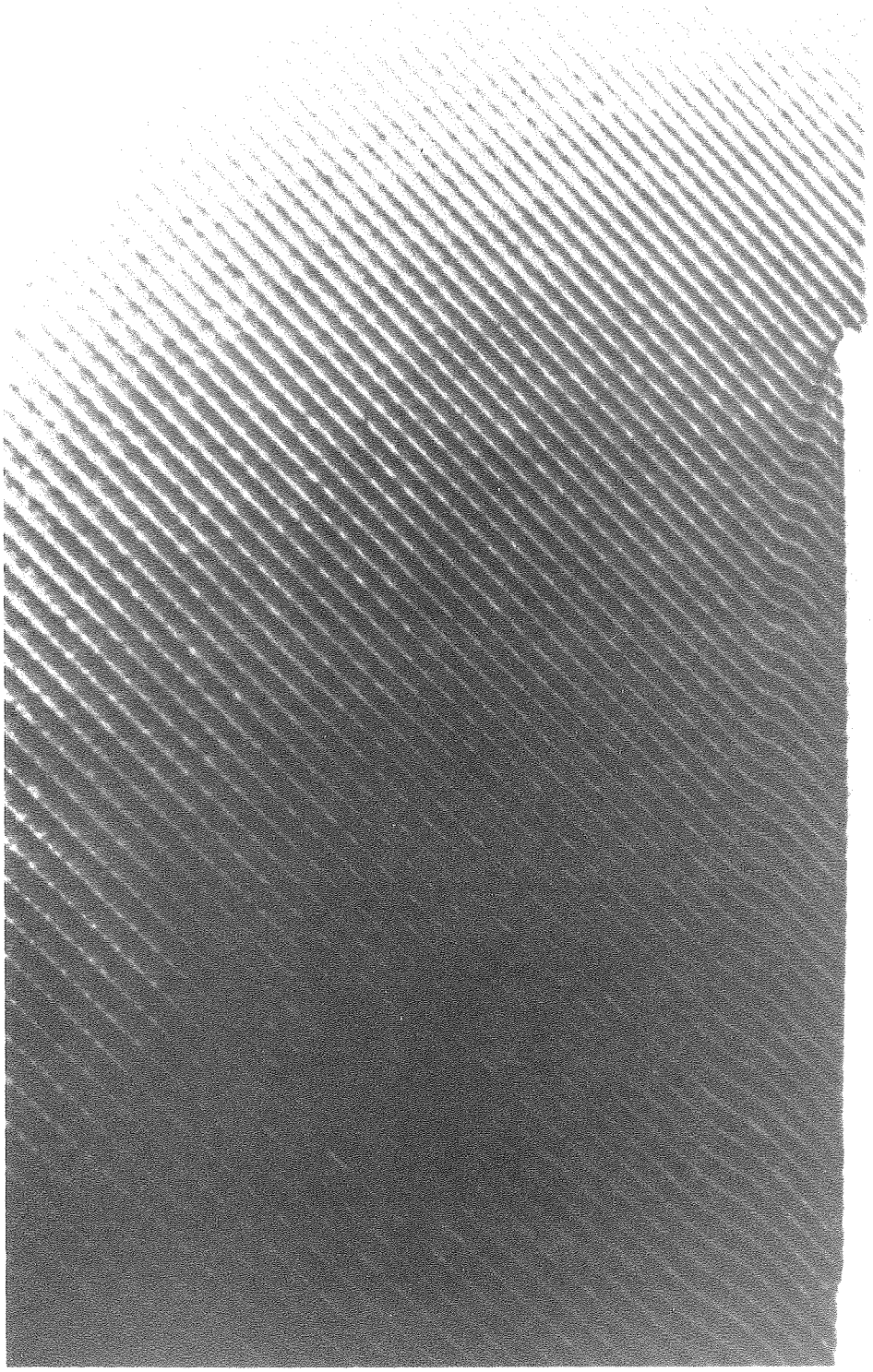

XBB 7710-9522

Figure 18. Deflection mapping photograph of the flat plate boundary layer. All variables are the same as in Fig. 17 except for the addition of hydrogen at 0.1 equivalence ratio. Note thicker boundary layer.

XBB 7710-9521

Figure 19. Deflection mapping photograph of the flat plate boundary layer. Variables are the same as in Fig. 18 except that the heating power for the first strip has been turned off. The temperature at the first strip is maintained by catalytic combustion of the hydrogen-air mixture.

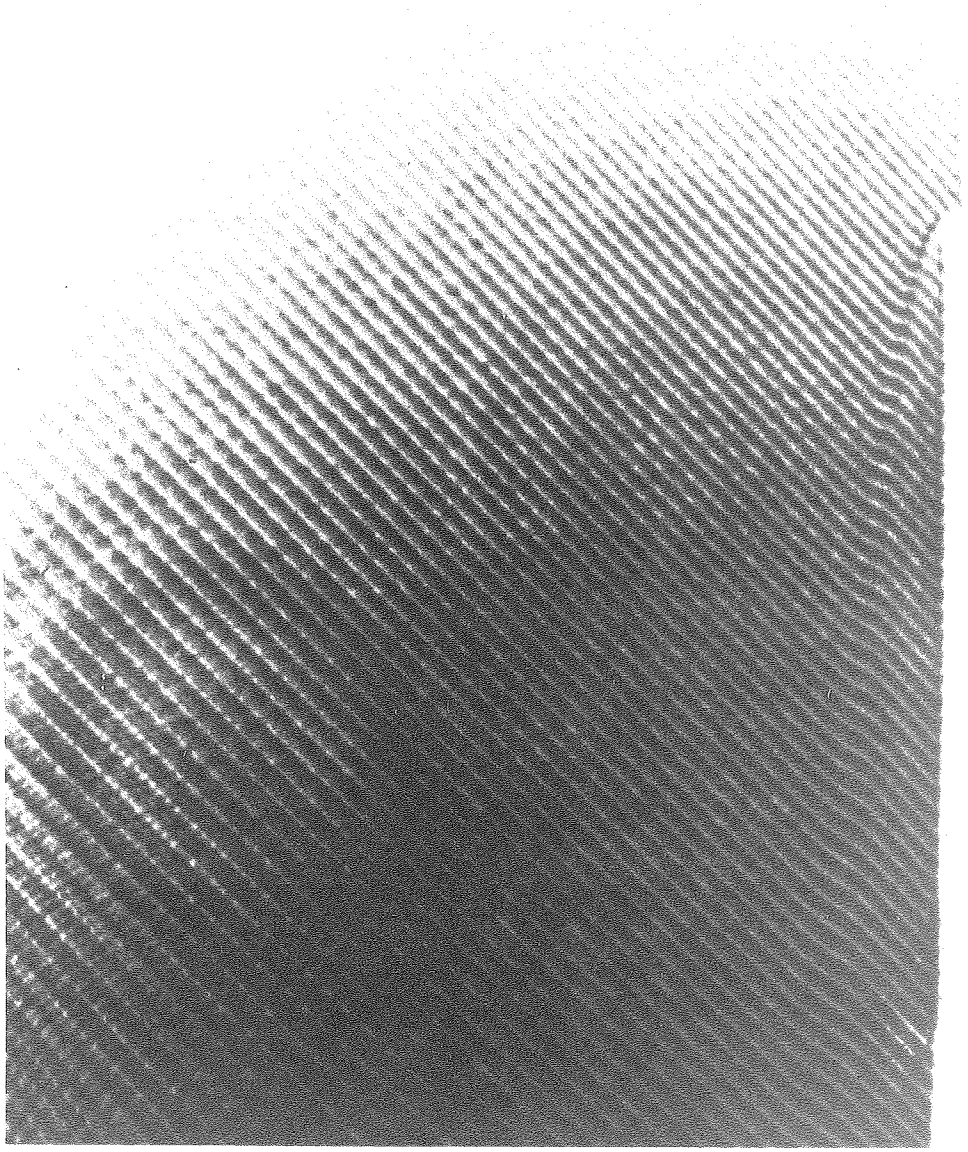

XBB 7710-9520

Figure 20. Deflection mapping photograph of the flat plate boundary layer. Flow is 0.2 equivalence ratio hydrogen-air mixutre, and there is no electrical heating power applied to the plate. Note rapid increase in boundary layer thickness about 10 mm downstream where the surface temperature jumps to a much larger value.

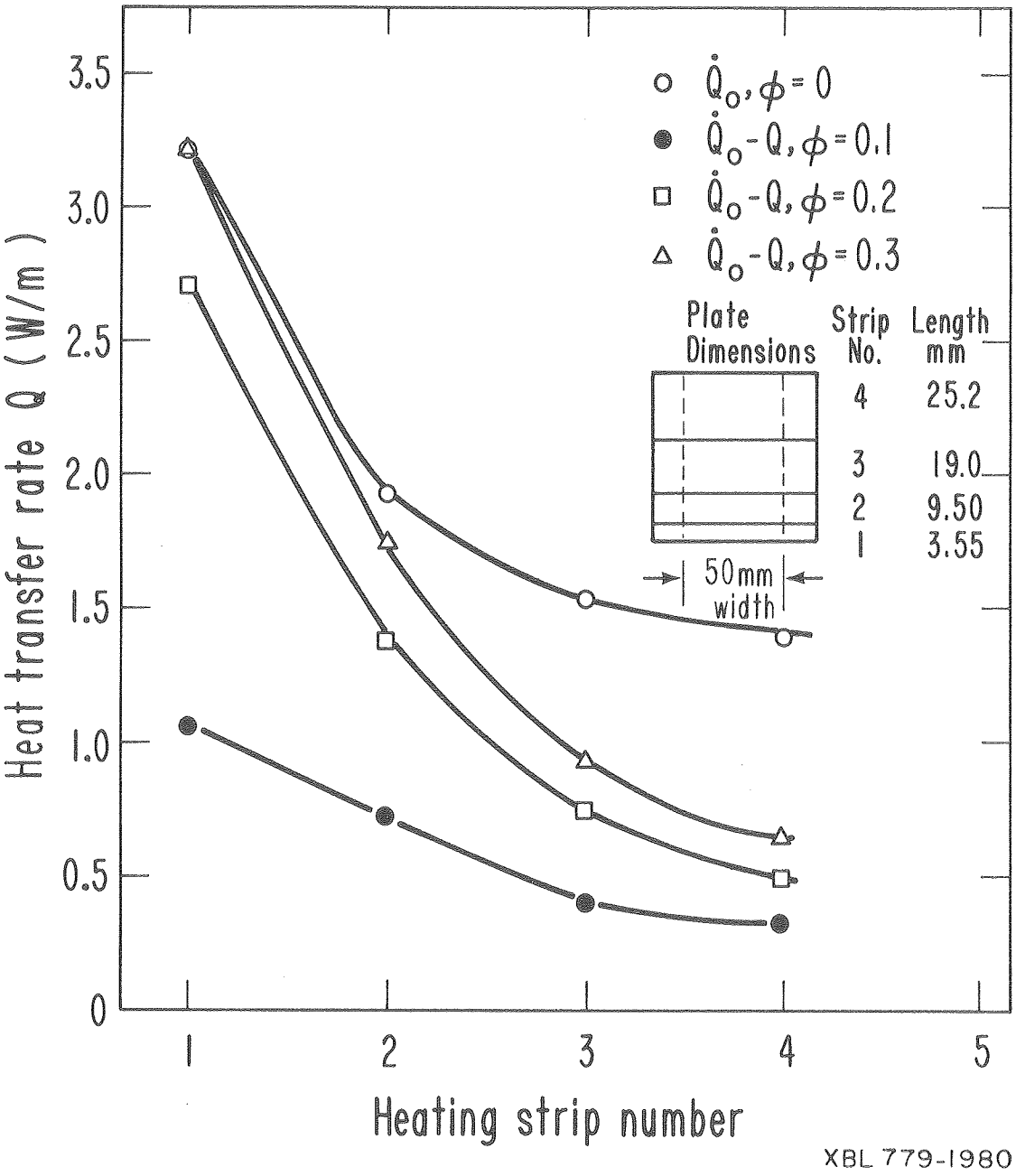

Figure 21. Drop in heating power for each strip as a function of hydrogen-air equivalence ratio. Platinum coated plate with surface temperature of 1130 K. Also shown is the heating power with no fuel (ϕ = 0).

This report was done with support from the United States Energy Research and Development Administration. Any conclusions or opinions expressed in this report represent solely those of the author(s) and not necessarily those of The Regents of the University of California, the Lawrence Berkeley Laboratory or the United States Energy Research and Development Administration.